

35. Jenkins PV, Dill JL, Zhou Q, et al. Clustered basic residues within segment 484–510 of the factor VIIIa A2 subunit contribute to the catalytic efficiency for factor Xa generation. *J Thromb Haemost.* 2004; 2: 452–458.
36. Fay PJ, Beattie T, Huggins CF, et al. Factor VIIIa A2 subunit residues 558–565 represent a factor IXa interactive site. *J Biol Chem* 1994; 269: 20522–20527.
37. Jenkins PV, Dill JL, Zhou Q, et al. Contribution of factor VIIIa A2 and A3-C1-C2 subunits to the affinity for factor IXa in factor Xase. *Biochemistry* 2004; 43: 5094–5101.
38. Fersht AR, Shi JP, Knill-Jones J, et al. Hydrogen bonding and biological specificity analysed by protein engineering. *Nature* 1985; 314: 235–238.
39. Pemberton S, Lindley P, Zaitsev V, et al. A molecular model for the triplicated A domains of human factor VIII based on the crystal structure of human ceruloplasmin. *Blood* 1997; 89: 2413–2421.
40. Church WR, Jernigan RL, Toole J, et al. Coagulation factors V and VIII and ceruloplasmin constitute a family of structurally related proteins. *Proc Natl Acad Sci USA* 1984; 81: 6934–6937.
41. Heeb MJ, Kojima Y, Hackeng TM, et al. Binding sites for blood coagulation factor Xa and protein S involving residues 493–506 in factor Va. *Protein Sci* 1996; 5: 1883–1889.
42. Fernández JA, Heeb MJ, Griffin JH. Identification of residues 413–433 of plasma protein S as essential for binding to C4b-binding protein. *J Biol Chem* 1993; 268: 16788–16794.
43. Linse S, Hårdig Y, Schultz DA, et al. A region of vitamin K-dependent protein S that binds to C4b binding protein (C4BP) identified using bacteriophage peptide display libraries. *J Biol Chem* 1997; 272: 14658–14665.
44. Heeb MJ, Kojima Y, Rosing J, et al. C-terminal residues 621–635 of protein S are essential for binding to factor Va. *J Biol Chem* 1999; 274: 36187–36192.

Identification of Plasmin-interactive Sites in the Light Chain of Factor VIII Responsible for Proteolytic Cleavage at Lys³⁶*

Received for publication, March 20, 2008, and in revised form, January 5, 2009. Published, JBC Papers in Press, January 6, 2009, DOI 10.1074/jbc.M802224200

Keiji Nogami^{†1}, Katsumi Nishiyama[‡], Evgueni L. Saenko[§], Masahiro Takeyama[‡], Kenichi Ogiwara[‡], Akira Yoshioka[‡], and Midori Shima[‡]

From the [†]Department of Pediatrics, Nara Medical University, Kashihara, Nara 634-8522, Japan and the [§]Department of Biochemistry and Molecular Biology, University of Maryland School of Medicine, Baltimore, Maryland 21201

We have recently reported that plasmin likely associates with the factor VIII light chain to proteolyze at Lys³⁶ within the A1 domain. In this study, we determined that the rate of plasmin-catalyzed inactivation on the forms of factor VIIIa containing A1-(1–336) and ¹⁷²²A3C1C2, reflecting Lys³⁶ cleavage, was reduced by ~60%, compared with those containing ¹⁶⁴⁹A3C1C2 and ¹⁶⁹⁰A3C1C2. SDS-PAGE analysis revealed that Lys³⁶ cleavage of factor VIIIa with ¹⁷²²A3C1C2 was markedly slower than those with ¹⁶⁴⁹A3C1C2 and ¹⁶⁹⁰A3C1C2. Surface plasmon resonance-based assays, using active site-modified anhydro-plasmin (Ah-plasmin) showed that ¹⁷²²A3C1C2 bound to Ah-plasmin with an ~3-fold lower affinity than ¹⁶⁴⁹A3C1C2 or ¹⁶⁹⁰A3C1C2 (K_D , 176, 68.2, and 60.3 nM, respectively). Recombinant A3 bound to Ah-plasmin (K_D , 44.2 nM), whereas C2 failed to bind, confirming the presence of a plasmin-binding site within N terminus of A3. Furthermore, the Glu-Gly-Arg active site-modified factor IXa also blocked ¹⁷²²A3C1C2 binding to Ah-plasmin by ~95%, supporting the presence of another plasmin-binding site overlapping the factor IXa-binding site in A3. In keeping with a major contribution of the lysine-binding sites in plasmin for interaction with the factor VIII light chain, analysis of the A3 sequence revealed two regions involving clustered lysine residues in 1690–1705 and 1804–1818. Two peptides based on these regions blocked ¹⁶⁴⁹A3C1C2 binding to Ah-plasmin by ~60% and plasmin-catalyzed Lys³⁶ cleavage of factor VIIIa with A1-(1–336) by ~80%. Our findings indicate that an extended surface, centered on residues 1690–1705 and 1804–1818 within the A3 domain, contributes to a unique plasmin-interactive site that promotes plasmin docking during cofactor inactivation by cleavage at Lys³⁶.

Factor VIII circulates as a complex with von Willebrand factor and functions as an essential cofactor in the tenase complex responsible for anionic phospholipid surface-dependent conversion of factor X to Xa by factor IXa (1). Molecular defects in factor VIII result in the congenital bleeding disorder, hemo-

philia A. Factor VIII is composed of 2,332 amino acid residues with a molecular mass of ~300 kDa and contains three types of structural domain, arranged in the order of A1-A2-B-A3-C1-C2 (2, 3). Mature factor VIII is processed to a series of metal ion-dependent heterodimers by cleavage at the B-A3 junction, generating a heavy chain consisting of the A1 and A2 domains, together with heterogeneous fragments of a partially proteolyzed B domain, linked to a light chain consisting of the A3, C1, and C2 domains (2–4).

Factor VIII is converted into an active form, factor VIIIa, by limited proteolysis catalyzed by either thrombin or factor Xa (5). Cleavages at Arg³⁷² and Arg⁷⁴⁰ in the heavy chain produce 50-kDa A1 and 40-kDa A2 subunits. Cleavage of the 80-kDa light chain (¹⁶⁴⁹A3C1C2) at Arg¹⁶⁸⁹ produces a 70-kDa A3C1C2 subunit (¹⁶⁹⁰A3C1C2). Additional cleavage by factor Xa at Arg¹⁷²¹ produces a 67-kDa A3C1C2 subunit (¹⁷²²A3C1C2). Proteolysis at Arg³⁷² and Arg¹⁶⁸⁹ is essential for generating factor VIIIa cofactor activity (6). Cleavage at the former site exposes a functional factor IXa-interactive site within the A2 domain that is cryptic in the unactivated molecule (7). Cleavage at the latter site liberates the cofactor from its carrier protein, von Willebrand factor (8), and contributes to the overall specific activity of the cofactor (9, 10).

APC² (5), factor Xa (5), and factor IXa (11) are serine proteases that inactivate factor VIII(a) by cleavage at Arg³³⁶ within the A1 subunit. This inactivation appears to be associated with an altered interaction between the A2 subunit and truncated A1 and is coupled with an increase in the K_m value for the substrate, factor X (12, 13), reflecting loss of a factor X-interactive site within residues 337–372 (14). In addition, a second specific cleavage site for factor Xa, Lys³⁶, was identified within the A1 subunit (13). Attack at this site also results in factor VIII inactivation mediated by an altered conformation of the A1 subunit limiting productive interaction with the A2 subunit (13).

Plasmin is a potent fibrinolytic protease and is composed of a heavy chain consisting of five kringle domains and a light chain containing the catalytic domain. The protease associates with numerous proteins via the LBS on the exposed surface (15). Several reports have shown that plasmin proteolytically inacti-

* This work was supported in part by Grant from MEXT KAKENHI 19591264 and Mitsubishi Pharma Research Foundation. An account of this work was presented at the 48th annual meeting of the American Society of Hematology, December 9, 2006, Orlando, FL. The costs of publication of this article were defrayed in part by the payment of page charges. This article must therefore be hereby marked "advertisement" in accordance with 18 U.S.C. Section 1734 solely to indicate this fact.

¹ To whom correspondence should be addressed: Dept. of Pediatrics, Nara Medical University, 840 Shijo-cho, Kashihara, Nara 634-8522, Japan. Tel.: 81-744-29-8881; Fax: 81-744-24-9222; E-mail: roc-noga@naramed-u.ac.jp.

² The abbreviations used are: APC, activated protein C; LBS, lysine-binding site; EGR-factor IXa, Glu-Gly-Arg active site-modified factor IXa; mAb, monoclonal antibody; rA3, recombinant A3; rC2, recombinant C2; Ah-plasmin, anhydro-plasmin; CAPS, 3-(cyclohexylamino)-1-propanesulfonic acid; SPR-based assay, surface plasmon resonance-based assay; ELISA, enzyme-linked immunosorbent assay.

vates several coagulation proteins, including factors Va (16, 17), VIII (18), IXa (19), and X (20). In detail, we have demonstrated that plasmin rapidly inactivates factor VIII by cleavage at Arg³³⁶ (18). Direct binding assays using Ah-plasmin, a catalytically inactive derivative of plasmin, revealed that plasmin interacts with the factor VIII heavy chain, predominantly the A2 domain, with high affinity ($K_d \sim 6$ and ~ 20 nM, respectively), in a mechanism largely independent of LBS (21). Our findings demonstrated, in particular, that Arg⁴⁸⁴ in the A2 domain significantly contributes to a unique plasmin-interactive site within the heavy chain that promotes plasmin docking during cleavage of the heavy chain (21).

In contrast, plasmin interacts with the factor VIII light chain with moderate affinity ($K_d \sim 70$ nM), predominantly through LBS-dependent mechanisms (21). Our previous data suggested that plasmin cleavage at Lys³⁶ within the A1 domain appears to be selectively regulated by the light chain (18). In this study, we have expanded our studies using truncated light chain, recombinant factor VIII subunits, and synthetic peptides, and identified plasmin-interactive sites within the light chain responsible for cleavage at Lys³⁶. Our results indicate that an extended surface centered on lysine residues involving the 1690–1705 and 1804–1818 regions in the A3 domain contributes to a unique plasmin-interactive site that promotes plasmin docking during cofactor inactivation by cleavage of the heavy chain at Lys³⁶.

MATERIALS AND METHODS

Reagents—Purified recombinant factor VIII preparations and the monoclonal antibody (mAb58.12) recognizing the N terminus of the A1 domain (22) were generous gifts from the Bayer Corp. (Osaka, Japan). The mAb NMC-VIII/5 recognizing the C2 domain was purified as described previously (23). Purified human plasmin (Lys-plasmin) devoid of factor Xa or APC was purchased from Sigma. Ah-plasmin, a catalytically inactive derivative of plasmin in which the active site serine is replaced by dehydroalanine, was prepared as described previously (21). The modified product demonstrated <1% plasmin activity, and its molecular weight was similar to that of native plasmin. Factor IXa, Glu-Gly-Arg active site-modified factor IXa (EGR-factor IXa), factor Xa, and thrombin were obtained from Hematologic Technologies Inc. (Essex Junction, VT). Pefabloc and horseradish peroxidase-labeled streptavidin were purchased from Roche Applied Science and Chemicon (Melbourne, Australia), respectively. Phospholipid vesicles containing 10% phosphatidylserine, 60% phosphatidylcholine, and 30% phosphatidylethanolamine (Sigma) were prepared using *N*-octyl glucoside (24). The mAb IgG preparations were biotinylated using *N*-hydroxysuccinimido-biotin reagent (Pierce). Synthetic peptides corresponding to factor VIII A3 residues 1690–1705 and 1804–1818 were prepared by BioSynthesis, Inc. (Lewisville, TX).

Isolation of Factor VIIIa Subunits—The intact light chain (¹⁶⁴⁹A3C1C2) and heavy chain were isolated from factor VIII following the SP- and Q-Sepharose chromatography (Amersham Biosciences) (7). The ¹⁶⁹⁰A3C1C2 and ¹⁷²²A3C1C2 subunits were purified from thrombin- and factor Xa-cleaved ¹⁶⁴⁹A3C1C2 subunit, respectively, following SP-Sepharose chromatography (10, 25). The A1-(1–372) subunit was purified

from thrombin-cleaved heavy chain using Mono Q columns (12). The A1-(1–336) and A1-(37–336) subunits were purified from APC- and factor Xa-cleaved A1 subunits, following SP- and chelate-Sepharose, respectively (13). Factor VIIIa was isolated from thrombin-cleaved factor VIII by CM-Sepharose chromatography (Amersham Biosciences) (27). SDS-PAGE and staining of the isolated subunits with GelCode Blue Stain Regent (Pierce) showed >95% purity. Protein concentrations were determined by the method of Bradford (28).

Expression and Purification of Recombinant A3 (rA3) and C2 (rC2) Domains—The rA3 domain of factor VIII (residues 1690–2019) was expressed in *Escherichia coli* using the pET expression system (Novagen, Madison, WI). The pMT2/factor VIII plasmid containing the B domain-deleted factor VIII gene (29) was obtained from Dr. Pipe (University of Michigan, Ann Arbor, MI). DNA fragments encoding the A3 domain were generated by PCR using pMT2/factor VIII as a template and a pair of corresponding primers. The amplified fragments were ligated with pET-20b(+) expression vectors. Plasmid DNA was purified, and the sequence was confirmed by direct sequencing in both directions using Applied Biosystems technology (Foster City, CA). The plasmid was used for transformation of Origami(DE3)pLysS *E. coli* cells (Novagen), the host strain for the protein expression. The protein was expressed and subsequently purified using a His-Select affinity cartridge (Sigma). Proper folding of the rA3 fragment was confirmed by determination of the affinities for conformationally sensitive anti-A3 mAb CLB-CAGa (30). The cDNA coding the C2 domain sequence of human factor VIII was constructed, transformed into *Pichia pastoris* cells, and expressed in a yeast secretion system as described previously (31). The rC2 protein was purified by ammonium sulfate fractionation and CM-Sepharose chromatography (Amersham Biosciences) as described previously (31).

Reconstitution of Factor VIIIa Form—The A1/A3C1C2 dimer was reconstituted by mixing 500 nM of A1 form (A1-(1–372), A1-(1–336), and A1-(37–336)) and an equimolar amount of A3C1C2 form (¹⁶⁴⁹A3C1C2, ¹⁶⁹⁰A3C1C2, and ¹⁷²²A3C1C2) overnight at 4 °C in 20 mM HEPES, pH 7.2, 0.3 M NaCl, 25 mM CaCl₂, and 0.01% Tween 20 (13). Furthermore, the reconstituted A1/A3C1C2 dimer forms (100 nM) were reacted with the excess amounts (300 nM) of A2 subunit for >15 min at 22 °C to minimize the A2 subunit dissociation from factor VIIIa. Reaction for >15 min generated the maximal factor VIIIa activity.

Factor Xa Generation Assay—The rate of conversion of factor X to factor Xa was monitored in a purified system (13). Plasmin-catalyzed inactivation of factor VIIIa was performed in HBS buffer (20 mM HEPES, pH 7.2, 0.1 M NaCl, 5 mM CaCl₂, 0.01% Tween 20) containing 0.1% bovine serum albumin and phospholipid vesicles (10 μM). Samples were removed from the mixtures at the indicated times, and plasmin reaction was immediately quenched by the addition of 0.2 mM Pefabloc and dilution. All reactions were performed at 37 °C. Factor Xa generation was initiated by the addition of factor IXa (20 nM) and factor X (400 nM) in the presence of phospholipid (10 μM). The reaction was quenched by addition of EDTA (100 mM). Rates of factor Xa generation were determined at 405 nm using a microtiter plate reader after the addition of chromogenic substrate,

Plasmin-interactive Sites in the Factor VIII Light Chain

S-2222 (0.46 nM final concentration). A control experiment showed that the presence of plasmin and Pefabloc in the diluted samples did not affect this assay (data not shown). Factor VIIIa activity was determined as the amount (in nanomoles) of factor Xa generated per min and converted into the amount (in nanomoles) of factor VIIIa.

Experiments assessing the stability of factor VIIIa were performed in the absence of plasmin to determine the rates of factor VIIIa activity loss resulting from the A2 dissociation. At the concentrations employed, ~5% loss of the initial activity was observed over a 20-min time course. Thus, for each time point in this experiment, including plasmin, the observed residual activity was corrected for the contribution of activity loss from the plasmin-independent mechanism.

Cleavage of Factor VIIIa Forms by Plasmin—Human plasmin (4 nM) was added to the reconstituted factor VIIIa forms (100 nM) at 37 °C in HBS buffer containing phospholipid vesicles (10 μM). Samples were obtained at the indicated times, and the reactions were immediately terminated and prepared for PAGE by adding SDS and 2-mercaptoethanol and boiling for 3 min.

Electrophoresis and Western Blotting—SDS-PAGE was performed using 8% gels by the procedure of Laemmli (32). Electrophoresis was carried out at 150 V for 1 h. For Western blotting, the proteins were transferred to a polyvinylidene difluoride membrane at 50 V for 2 h in buffer containing 10 mM CAPS, pH 11, and 10% (v/v) methanol. Proteins were probed using anti-A1 mAb58.12, followed by goat anti-mouse peroxidase-linked secondary antibody (MP Biomedicals, Aurora, OH). The signals were detected using the enhanced chemiluminescence system (PerkinElmer Life Sciences).

Kinetics Measurements Using Real Time Biomolecular Interaction Analysis—The kinetics of factor VIII light chain and plasmin interaction were determined by SPR-based assays using a BIAcore X instrument (BIAcore AB, Uppsala, Sweden) as reported previously (21). Ah-plasmin was covalently coupled (~7 ng/mm²) to a CM5 sensor chip surface. Association of the ligand was monitored at a flow rate of 20 μl/min for 4 min. The dissociation of bound ligand was recorded over a 4-min period by replacing the ligand-containing buffer with buffer alone. The level of nonspecific binding corresponding to ligand binding to the uncoated chip was subtracted from the signal. The reactions were run at 37 °C. The rate constants for association (k_a) and dissociation (k_d) were determined by nonlinear regression analysis using the evaluation software provided by BIAcore AB. Equilibrium dissociation constants (K_d) were calculated as k_d/k_a .

ELISA Binding Assays Using Immobilized Ah-plasmin—These assays were performed as reported previously (21). Briefly, Ah-plasmin (200 nM) was coated onto microtiter wells overnight at 4 °C. The wells were blocked with 5% bovine serum albumin for 2 h at 37 °C, and various concentrations of the A3C1C2 subunits were added and incubated for 2 h at 37 °C. Biotinylated anti-C2 NMC-VIII/5 mAb IgG (1 μg) was added to each well, and bound IgG was detected by addition of horseradish peroxidase-labeled streptavidin. The absorbance was measured at 492 nm with a Labsystems Multiskan Multisoft microplate reader (Labsystems, Helsinki, Finland). The amount of nonspecific binding of biotinylated IgG, observed in the

absence of A3C1C2, was <5% of the total signal, and the amount of specific binding was obtained by subtracting the amount of nonspecific binding of biotinylated IgG.

Data Analysis—All experiments were performed at least three separate times. The parameters and their standard errors are shown. Nonlinear least squares or linear regression analysis was performed by KaleidaGraph (Synergy Reading, PA). The rates of the slope of first several points (within 5 min) in the time course of the plasmin-catalyzed inactivation of factor VIIIa form were fitted to a straight line from linear regression, and the obtained values were expressed as the inactivation rate. All correlation values (r) were >0.99.

Analyses of the interactions between the different forms of A3C1C2 and Ah-plasmin in ELISA were performed by a single-site binding model using Equation 1,

$$A = \frac{A_{\max} \cdot [S]}{K_d + [S]} \quad (\text{Eq. 1})$$

where [S] is the concentration of A3C1C2 form in the solid-phase binding assay; K_d is the dissociation constant; and A_{\max} represents maximum absorbance signal when the site is saturated by the A3C1C2 form.

Data from studies assessing the EGR-factor IXa or A3 synthetic peptide-dependent inhibition of plasmin interaction with A3C1C2 form were fitted by nonlinear least squares regression by using Equation 2,

$$\% \text{ binding} = \frac{B_{\max} \cdot [\text{A3C1C2 form}]}{K_d \cdot \left(1 + \frac{[L]}{K_i}\right) + [\text{A3C1C2 form}]} + C \quad (\text{Eq. 2})$$

where L represents the concentration of EGR-factor IXa or A3 peptide; B_{\max} represents maximum binding; K_d is the dissociation constant for the interaction between the A3C1C2 form and Ah-plasmin; K_i is the apparent inhibition constant for L ; and C is a constant for binding of the A3C1C2 form and Ah-plasmin that was unaffected by L .

RESULTS

Plasmin-catalyzed Inactivation of Factor VIIIa Reconstituted with the A1¹⁻³³⁶ and Various A3C1C2 Forms—We have recently reported that plasmin appears to associate with the light chain of factor VIII to regulate the proteolytic cleavage at Lys³⁶ within the A1 subunit by its protease (18). To investigate whether the light chain contributes to plasmin-catalyzed factor VIIIa inactivation because of Lys³⁶ cleavage, we first examined the effect on plasmin-catalyzed inactivation of factor VIIIa forms reconstituted with various A3C1C2 forms. Intact A1-(1-372) subunit is proteolyzed at Arg³³⁶ and Lys³⁶ by plasmin, and the former cleavage significantly contributes to the factor VIIIa inactivation (18). Therefore, the A1-(1-336) subunit was utilized instead of the A1-(1-372) to observe the effect of Lys³⁶ cleavage alone. Factor VIIIa forms were reconstituted in two-step procedures. The A1-(1-336)/A3C1C2 dimer forms were prepared by reacting the equimolar concentrations (500 nM) of the A1-(1-336) and isolated A3C1C2 subunits (¹⁶⁴⁹A3C1C2,

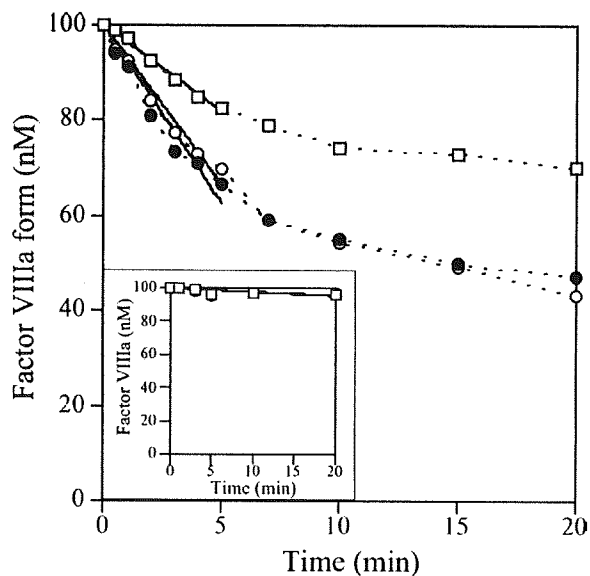


FIGURE 1. Plasmin-catalyzed inactivation of factor VIIIa forms reconstituted with various A1 and A3C1C2 subunits. The A1-(1-336) or A1-(37-336) (*inset*) subunit was reconstituted with the 1649 A3C1C2 (*open circles*), 1690 A3C1C2 (*closed circles*), and 1722 A3C1C2 (*open squares*) subunits as described under "Materials and Methods." The A1/A3C1C2 dimers (100 nM) were reacted with the A2 subunit (300 nM) and phospholipid vesicles (10 μ M). Factor VIIIa inactivation was then monitored over time in the presence of plasmin (1 nM) using a factor Xa generation assay. Plasmin-catalyzed inactivation values were corrected by subtracting the corresponding values for factor VIIIa decay observed in the absence of plasmin. *Solid lines* were drawn from the linear regression fitting to evaluate the rate of plasmin-catalyzed inactivation of factor VIIIa with A1-(1-336) or A1-(37-336).

1690 A3C1C2, and 1722 A3C1C2) in the presence of Ca^{2+} . The resultant dimers were diluted 5-fold and reacted with the A2 subunit (300 nM) to generate factor VIIIa heterotrimers. The A2 subunit was used at higher concentration to minimize its inactivation because of A2 dissociation from A1/A3C1C2 dimer. Inactivation of various factor VIIIa forms were then monitored over time in the presence of plasmin (1 nM) and phospholipid vesicles (10 μ M) using a factor Xa generation assay as described under "Materials and Methods." The presence of plasmin and Pefabloc in the diluted samples did not affect this assay (data not shown). These data are illustrated in Fig. 1 and Table 1.

In the absence of plasmin, the maximal generated factor Xa obtained at saturable levels of reconstituted factor VIIIa with A1-(1-336) and the loss (decay) of its activity were similar (V_{\max} , ~ 55 nM/min and $\sim 5\%$ activity loss at 20 min, respectively), independent of various A3C1C2 forms (data not shown). The activity of factor VIIIa forms with 1649 A3C1C2 subunit was rapidly reduced in a time-dependent manner by the addition of plasmin, similar to that of factor VIIIa with 1690 A3C1C2, with similar inactivation rates. The reduced activity reached $\sim 55\%$ of initial activity at 20 min. Of interest, slower inactivation of factor VIIIa with 1722 A3C1C2 by plasmin was observed, compared with 1649 A3C1C2 and 1690 A3C1C2. The activity was reduced by $\sim 30\%$ at 20 min, and the inactivation rate was $\sim 45\%$ that observed with 1649 A3C1C2 and 1690 A3C1C2. These results suggested that the N terminus of the

TABLE 1

Rates of plasmin-catalyzed inactivation of factor VIIIa forms reconstituted with various A1 and A3C1C2 forms

Inactivation of factor VIIIa forms was estimated by the rate obtained using the straight line fitting by the first several points (within 5 min) of the data shown in Fig. 1. Data points represent mean \pm S.D. values of at least three separate experiments.

| A3C1C2 form | A1 form | |
|------------------|---------------------------|----------------------|
| | A1 ¹⁻³³⁶ | A1 ³⁷⁻³³⁶ |
| | <i>Inactivation rates</i> | |
| 1649 A3C1C2 | 7.8 \pm 0.2 | 0.2 \pm 0.04 |
| 1690 A3C1C2 | 7.9 \pm 0.4 | 0.2 \pm 0.05 |
| 1722 A3C1C2 | 3.4 \pm 0.2 | 0.2 \pm 0.03 |

light chain might be associated with plasmin-catalyzed inactivation of factor VIIIa with A1-(1-336) mediated by cleavage at Lys³⁶.

To further examine that inactivation of factor VIIIa with A1-(1-336) subunit by plasmin attributed to Lys³⁶ cleavage, we repeated the same experiments using factor VIIIa forms reconstituted with the A1-(37-336) subunit, deleting the A1-(1-36). Factor VIIIa forms with the A1-(37-336), and various A3C1C2 subunits were reconstituted by the same approach. Independent of A3C1C2 forms, the maximally generated factor Xa and the activity loss (decay) of factor VIIIa forms were similar (V_{\max} , ~ 25 nM/min and $\sim 5\%$ activity loss, respectively) in the absence of plasmin (data not shown). Three factor VIIIa forms with A1-(37-336) were, however, little inactivated (by $\sim 5\%$) by plasmin even at over a 20-min reaction (Fig. 1, *inset*). Inactivation rates were similar, supporting the view that plasmin-catalyzed inactivation of factor VIIIa with A1-(1-336) subunit was regulated by Lys³⁶ cleavage.

Addition of Various A3C1C2 Forms on Plasmin-catalyzed Inactivation of Factor VIIIa with A1¹⁻³³⁶—To confirm that the N terminus of the A3C1C2 domain is responsible for plasmin-catalyzed inactivation of factor VIIIa, we examined the inhibitory effects by the addition of various A3C1C2 forms on these reactions. The A1-(1-336)/ 1649 A3C1C2 dimer was reconstituted with excess amounts of A2 subunit, and factor VIIIa inactivation was then monitored by the addition of plasmin (1 nM) in the presence of various A3C1C2 in a factor Xa generation assay as described under "Materials and Methods." The presence of competitors, A3C1C2 forms, did not affect this assay (data not shown). These data are illustrated in Fig. 2 and Table 2. The addition of the 1649 A3C1C2 and 1690 A3C1C2 subunits, rA3 domain (residues 1690–2019) (75 nM), each similarly inhibited plasmin-catalyzed inactivation of factor VIIIa with A1-(1-336), with an $\sim 55\%$ decrease in inactivation rate. Furthermore, the addition of a higher concentration (250 nM) of these A3C1C2 forms showed $\sim 90\%$ decreases in inactivation rates. In contrast, in the presence of 1722 A3C1C2, the inactivation rates were reduced by ~ 30 and $\sim 55\%$ at both concentrations, respectively, and the inhibitory effects were less than those of the other three A3C1C2 forms. The presence of rC2 domain (residues 2174–2332) had little effect. Taken together, these findings indicated that the 1690–1721 region in the A3 domain contributed to plasmin-catalyzed inactivation of factor VIIIa through Lys³⁶ cleavage.

Effects of the A3C1C2 Forms on Plasmin-catalyzed Cleavage at Lys³⁶ within the A1 Domain—To evaluate visually the effect of the various A3C1C2 forms on cleavage by plasmin at Lys³⁶ in

Plasmin-interactive Sites in the Factor VIII Light Chain

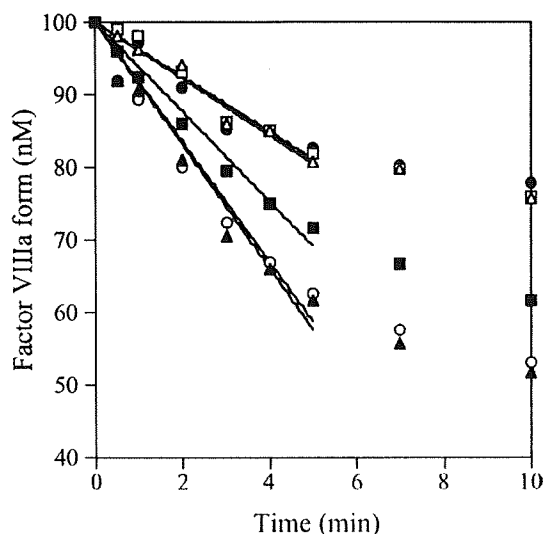


FIGURE 2. Effects of the addition of A3C1C2 form on plasmin-catalyzed inactivation of factor VIIIa forms with A1¹⁻³³⁶. Reconstituted A1-(1-336)/¹⁶⁴⁹A3C1C2 dimer (100 nM) reacted with the A2 subunit (300 nM) and phospholipid vesicles (10 μ M). Factor VIIIa inactivation was then monitored over time in the presence of various A3C1C2 forms (75 nM) and plasmin (1 nM) using a factor Xa generation assay. The symbols used are as follows: open circles, no A3C1C2; closed circles, ¹⁶⁴⁹A3C1C2; open squares, ¹⁶⁹⁰A3C1C2; closed squares, ¹⁷²²A3C1C2; open triangles, A3; closed triangles, C2. Plasmin-catalyzed inactivation values were corrected by subtracting the corresponding values for factor VIIIa decay observed in the absence of plasmin. Solid lines were drawn from the linear regression fitting to evaluate the rate of plasmin-catalyzed inactivation of factor VIIIa with A1-(1-336).

TABLE 2

Rates of plasmin-catalyzed inactivation of factor VIIIa with A1¹⁻³³⁶ by the addition of exogenous A3C1C2 forms

Inactivation of factor VIIIa forms was estimated by the rate obtained using the straight line fitting by the first several points (within 5 min) of the data shown in Fig. 2. Data points represent mean \pm S.D. values of at least three separate experiments.

| Amounts | Addition of exogenous A3C1C2 form | | | | |
|---------|-----------------------------------|------------------------|------------------------|---------------|---------------|
| | ¹⁶⁴⁹ A3C1C2 | ¹⁶⁹⁰ A3C1C2 | ¹⁷²² A3C1C2 | RA3 | rC2 |
| nM | Inactivation rates | | | | |
| 0 | 8.0 \pm 0.4 | 8.0 \pm 0.4 | 8.0 \pm 0.4 | 8.0 \pm 0.4 | 8.0 \pm 0.4 |
| 75 | 3.7 \pm 0.2 | 3.6 \pm 0.2 | 5.8 \pm 0.2 | 3.7 \pm 0.1 | 8.1 \pm 0.2 |
| 250 | 0.7 \pm 0.2 | 0.8 \pm 0.2 | 3.7 \pm 0.3 | 0.6 \pm 0.2 | 7.9 \pm 0.3 |

the A1 subunit, the A1-(1-372)/A3C1C2 dimer forms (¹⁶⁴⁹A3C1C2, ¹⁶⁹⁰A3C1C2, and ¹⁷²²A3C1C2) were reconstituted with the A2 subunit by the same approach. Factor VIIIa forms were then incubated with plasmin (4 nM), followed by Western blotting analyses using anti-A1 mAb58.12 for detection (Fig. 3A). This antibody recognizes the N-terminal region of A1, and the failure to detect the A1-(1-336) fragment indicates complete cleavage at Lys³⁶ and conversion to A1-(37-336) (18). In addition, the ratio of the A1-(1-336) product (at each time point) to the A1-(1-372) substrate (at time zero) was evaluated by scanning densitometry of the bands (Fig. 3B). In control experiments using isolated A1-(1-372) alone, the A1-(1-336) fragment was generated in a time-dependent manner within 20 min, indicating relatively slow cleavage by plasmin at Lys³⁶ (Fig. 3A, panel a). In contrast, with A1/¹⁶⁴⁹A3C1C2 (Fig. 3A, panel b) and A1/¹⁶⁹⁰A3C1C2 (panel c), the A1-(1-336) fragments were very weakly visualized, sug-

gesting almost complete cleavage by plasmin at Lys³⁶. Interestingly, with the A1/¹⁷²²A3C1C2 (Fig. 3A, panel d), the A1-(1-336) fragment appeared to be derived in a time-dependent manner within 10 min and then subsequently diminished. These findings suggested that cleavage at Lys³⁶ in the A1/¹⁷²²A3C1C2 was much slower than that with A1/¹⁶⁴⁹A3C1C2 or A1/¹⁶⁹⁰A3C1C2 but was faster than that with A1 alone. The data indicated that residues 1690-1721 in the A3 domain contain a site contributing to plasmin-catalyzed cleavage at Lys³⁶ in the A1 domain.

Binding of the A3C1C2 Forms to Ah-plasmin—A series of experiments were designed to assess plasmin binding to the A3C1C2 subunit to obtain direct evidence that the A3 domain contains a plasmin-interactive site that contributes to enzyme docking and facilitates catalysis of cleavage at Lys³⁶ in the A1 domain. In these experiments, Ah-plasmin, an active site-modified plasmin lacking enzymatic activity, was utilized, and this interaction was evaluated in a real time SPR-based assay. We have recently examined the interaction of Ah-plasmin and the factor VIII heavy chain using this technique (21). Varying amounts of A3C1C2 forms were applied to Ah-plasmin immobilized on a sensor chip. Fig. 4A shows a representative signal corresponding to association and dissociation of immobilized Ah-plasmin with ¹⁶⁴⁹A3C1C2 (panel a), ¹⁷²²A3C1C2 (panel b), and rA3 subunits (panel c). Binding parameters are summarized in Table 3. The data could be comparatively well fitted by nonlinear regression using a 1:1 Langmuir binding model. The rA3 domain and ¹⁶⁴⁹A3C1C2 and ¹⁶⁹⁰A3C1C2 subunits bound to Ah-plasmin. The resulting kinetic constants derived from the association and/or dissociation kinetic curves showed that the rA3 domain bound to Ah-plasmin with similar affinity to those of the ¹⁶⁴⁹A3C1C2 and ¹⁶⁹⁰A3C1C2 subunits (K_d , 44.2, 68.2, and 60.3 nM, respectively). The rC2 domain failed to bind. However, the ¹⁷²²A3C1C2 subunit bound with an \sim 3-fold lower affinity (K_d , 176 nM) than that obtained with ¹⁶⁹⁰A3C1C2. These data demonstrated that the A3 domain, especially residues in the 1690-1721 region, plays a significant role in the interaction with plasmin.

Our experiments utilizing the factor VIIIa with various A3C1C2 forms as substrate suggested that the N terminus of the A3 domain contains the predominant region contributing to plasmin-catalyzed cleavage at Lys³⁶. To confirm that the inhibition of plasmin cleavage at Lys³⁶ was mediated by the association between the dimer and plasmin, binding experiments with A1/A3C1C2 dimers were further examined. Both of the A1 dimers with ¹⁶⁴⁹A3C1C2 and ¹⁶⁹⁰A3C1C2 bound to Ah-plasmin with similar affinities (K_d , 26.9 and 32.9 nM, respectively), and these affinities were \sim 2.5-fold higher than those with either form of A3C1C2 alone. This somewhat higher affinity may have been derived from a synergistic effect of the two binding domains and/or a conformational change resulting from interaction with the two domains. However, the A1/¹⁷²²A3C1C2 dimer bound with an \sim 4-fold weaker affinity (K_d , 124 nM) than with the other dimers, and the isolated A1 alone bound very poorly (K_d , \sim 200 nM). The findings therefore suggest that residues 1690-1721 are indeed involved in a plasmin-binding site for cleavage at Lys³⁶.

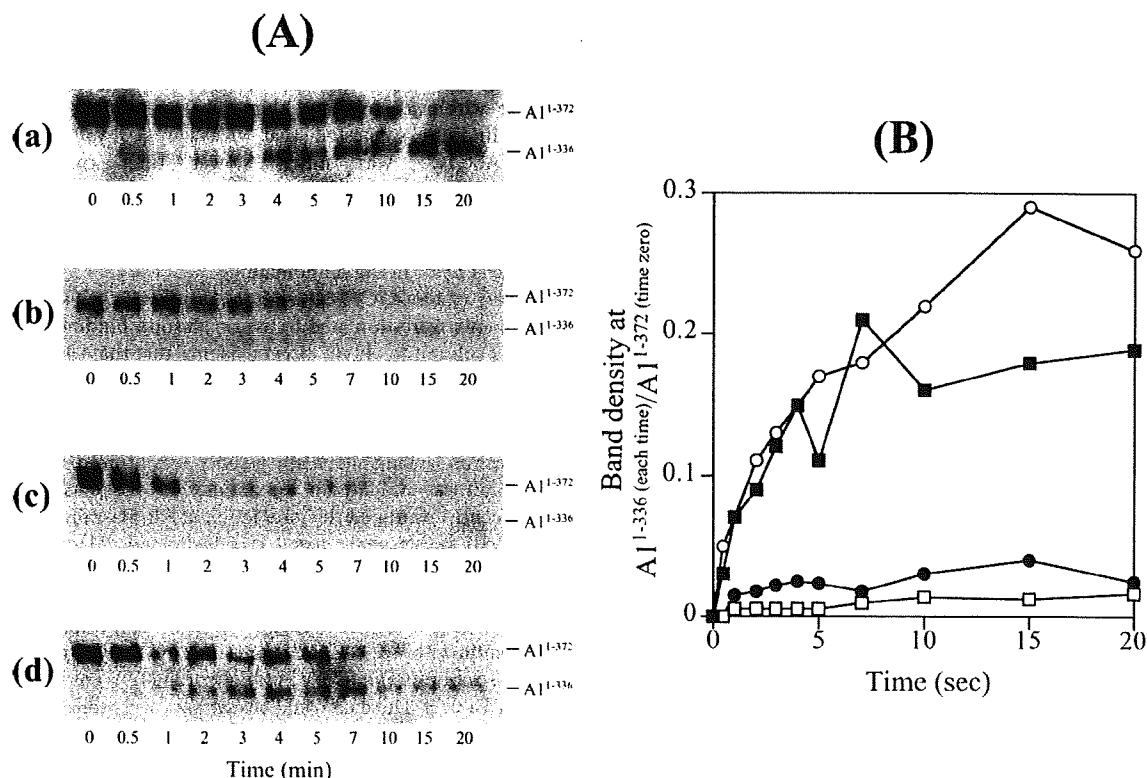


FIGURE 3. The contribution of A3C1C2 forms on cleavage by plasmin at Lys³⁶ in A1. A, A1 subunit (500 nM) was reconstituted with either equimolar buffer alone (panel a), ¹⁶⁴⁹A3C1C2 (panel b), ¹⁶⁹⁰A3C1C2 (panel c), or ¹⁷²²A3C1C2 (panel d) subunits as described under "Materials and Methods." After dilution, each dimer form (100 nM) was reacted with the A2 subunit (300 nM), followed by incubation with plasmin (4 nM) in the presence of phospholipid vesicles (10 μM) for the indicated times. Samples were analyzed on 8% gels followed by Western blotting using an anti-A1 (58.12) IgG. B shows quantitative densitometry of the ratio of (A1-1-336) at each time/(A1-1-372) at time 0 from blotting data obtained from A. The symbols used are as follows: open circles, A1 alone; closed circles, A1/¹⁶⁴⁹A3C1C2; open squares, A1/¹⁶⁹⁰A3C1C2; and closed squares, A1/¹⁷²²A3C1C2.

We further evaluated the interaction between the A3C1C2 subunit and plasmin using a solid-phase binding assay in which Ah-plasmin was immobilized onto microtiter wells. For these experiments, varying amounts of the A3C1C2 subunits were reacted with 200 nM immobilized Ah-plasmin. Bound factor VIII was detected using biotinylated anti-C2 NMC-VIII/5 mAb. Control experiments confirmed that this mAb did not affect the reaction between plasmin and the light chain (data not shown). Results are presented in Fig. 4B. Reactions between the A3C1C2 forms and Ah-plasmin yielded saturable binding curves, well fitted using a single-binding site model. This method is not based on a true equilibrium binding assay, however, and the K_d values obtained represent an apparent K_d value for the interactions. The results obtained for the ¹⁶⁴⁹A3C1C2 and the ¹⁶⁹⁰A3C1C2 subunits binding to Ah-plasmin were 97 ± 10 and 89 ± 9 nM, respectively, similar to those obtained in the SPR-based assays. However, the binding affinity (265 ± 21 nM) for the ¹⁷²²A3C1C2 subunit was ~3-fold lower than that for the two other forms. Again, the rC2 domain failed to bind. Overall, the affinities determined using the ELISA-based assays were in good agreement with those obtained in the SPR-based analyses, and the findings were mutually supportive.

Effect of Factor IXa on A3C1C2 Form Binding to Ah-plasmin—Our solid-phase binding assays demonstrated that the

¹⁷²²A3C1C2 subunit bound to Ah-plasmin, albeit with relatively weak affinity. These data led us to speculate on the presence of another plasmin-interactive site(s) in the A3 domain. We have recently shown that factor IXa inhibited plasmin-catalyzed inactivation of factor VIIIa, and we identified overlapping binding sites for plasmin and factor IXa in the A2 domain of factor VIII(a) (21). It is known that residues 1804–1818 in the A3 domain of factor VIII interact with factor IXa on phospholipid surfaces (30), and we therefore investigated the inhibitory effect of factor IXa on the light chain binding to Ah-plasmin in our ELISA method. The ¹⁶⁴⁹A3C1C2 subunit (120 nM) was mixed with varying amounts of active site-modified EGR-factor IXa for 1 h prior to incubation with Ah-plasmin (200 nM) immobilized onto microtiter wells. Bound ¹⁶⁴⁹A3C1C2 was detected using biotinylated anti-C2 mAb. EGR-factor IXa blocked ¹⁶⁴⁹A3C1C2 subunit binding to Ah-plasmin by ~40% at the maximum concentrations employed (500 nM), and this effect was dose-dependent (Fig. 5). The apparent K_i value for factor IXa obtained from curve fitting was 160 ± 51 nM. The association between the factor VIII light chain and factor IXa is surface-dependent, however (25), and hence the effects of factor IXa in our current binding studies were also examined in the presence of phospholipid. EGR-factor IXa blocked binding in a dose-dependent manner, and the inhibitory effect (~60%) was

Plasmin-interactive Sites in the Factor VIII Light Chain

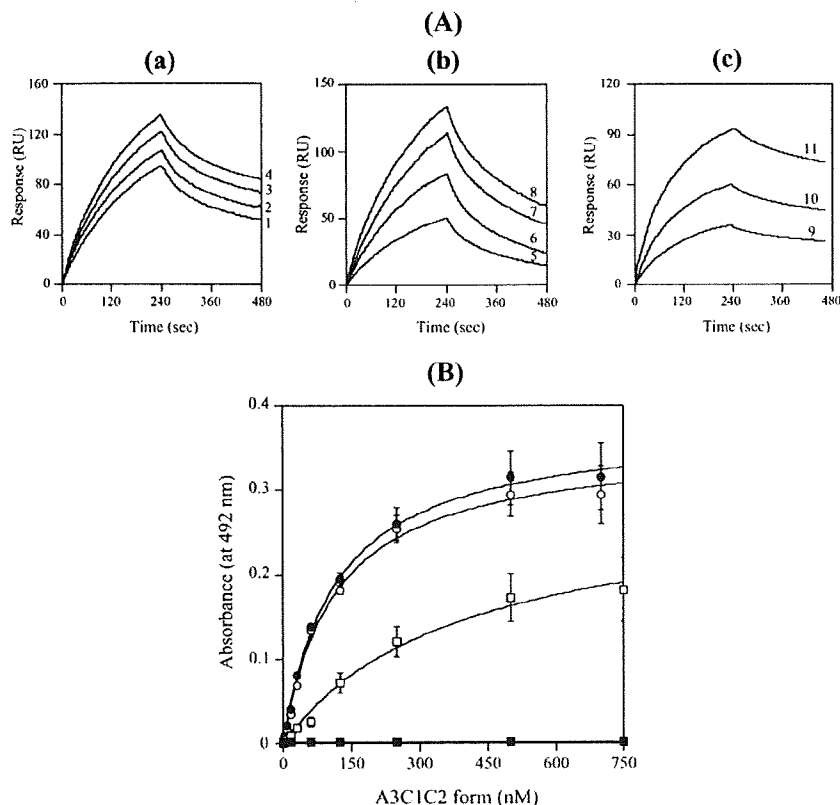


FIGURE 4. Direct binding of the A3C1C2 forms to Ah-plasmin. A, SPR-based assay. Various concentrations of $^{1649}\text{A3C1C2}$ (panel a), $^{1722}\text{A3C1C2}$ (panel b), and rA3 (panel c) were added to Ah-plasmin ($\sim 7 \text{ ng/mm}^2$) immobilized on the sensor chip for 4 min, followed by a change of running buffer for 4 min as described under "Materials and Methods." Lines 1–4 show response curves for $^{1649}\text{A3C1C2}$ (50, 100, 150, and 180 nM, respectively); lines 5–8 show curves for $^{1722}\text{A3C1C2}$ (50, 100, 200, and 300 nM, respectively); and lines 9–11 show curves for rA3 (60, 120, and 240 nM, respectively). B, ELISA-based assay. Various concentrations of $^{1649}\text{A3C1C2}$ (open circles), $^{1690}\text{A3C1C2}$ (closed circles), $^{1722}\text{A3C1C2}$ (open squares), and rC2 (closed squares) were incubated with Ah-plasmin (200 nM) that had been bound to microtiter wells. Bound A3C1C2 forms were detected using biotinylated anti-C2 (NMC-VIII/5) mAb IgG. Absorbance values were plotted as a function of the concentration of the A3C1C2 form, and the data were fitted using Equation 1 according to the single site binding model described under "Materials and Methods."

TABLE 3
Binding parameters of factor VIII A3C1C2 forms and Ah-plasmin in an SPR-based assay

Reactions were performed as described under "Materials and Methods." Parameter values were calculated by nonlinear regression analysis in Fig. 4A using the evaluation software provided by BIACore AB.

| Ligands | k_{on} | k_{off} | K_d^a |
|----------------------------|--------------------------------------|--------------------------|---------|
| | $10^3 \text{ M}^{-1} \text{ s}^{-1}$ | 10^{-3} s^{-1} | nM |
| Factor VIII | 26.3 ± 0.8 | 0.8 ± 0.1 | 3.1 |
| $^{1649}\text{A3C1C2}$ | 2.9 ± 0.5 | 2.0 ± 0.7 | 68.2 |
| $^{1690}\text{A3C1C2}$ | 4.9 ± 1.3 | 2.9 ± 0.5 | 60.3 |
| $^{1722}\text{A3C1C2}$ | 4.5 ± 2.3 | 7.9 ± 2.2 | 176 |
| A3 | 3.9 ± 0.3 | 1.7 ± 0.3 | 44.2 |
| C2 | ND ^b | ND | |
| A1/ $^{1649}\text{A3C1C2}$ | 7.8 ± 2.4 | 2.1 ± 0.6 | 26.9 |
| A1/ $^{1690}\text{A3C1C2}$ | 7.0 ± 1.6 | 2.3 ± 0.5 | 32.9 |
| A1/ $^{1722}\text{A3C1C2}$ | 4.9 ± 1.1 | 6.1 ± 1.2 | 124 |
| A1 | 5.2 ± 0.4 | 10.9 ± 0.9 | 208 |

^a Values were calculated as k_{off}/k_{on} .

^b ND indicates not determined.

greater than that in the absence of phospholipid. Furthermore, the K_d value ($10.5 \pm 1.5 \text{ nM}$) obtained from curve fitting was ~ 15 -fold lower in the presence of phospholipid than that in its

absence. These values were similar to the K_d values for light chain and factor IXa association in the presence and absence of phospholipid determined in a fluid-phase model (25).

It was evident, however, that inhibition of the interaction between $^{1649}\text{A3C1C2}$ and plasmin mediated by EGR-factor IXa was only partial ($\sim 60\%$), and to exclude the possibility that the 1690–1721 region in A3 contributed to the binding reaction in these experiments, we repeated the assays using the $^{1722}\text{A3C1C2}$ subunit (240 nM), instead of the nontruncated A3C1C2. EGR-factor IXa blocked the binding of $^{1722}\text{A3C1C2}$ subunit to Ah-plasmin by ~ 95 and $\sim 80\%$ in the presence and absence of phospholipid, respectively, at the maximum concentrations employed (Fig. 5). The calculated K_i values for factor IXa obtained from curve fitting were 9.8 ± 1.1 and $179 \pm 23 \text{ nM}$, respectively. This significant competitive reaction between factor IXa and $^{1722}\text{A3C1C2}$ for binding to plasmin therefore suggested that an alternative plasmin-interactive site in the factor VIII light chain, within residues 1804–1818 in the A3 domain, might overlap or juxtapose the factor IXa-binding site.

Binding of the 1690–1705 and 1804–1818 Peptides to Ah-plasmin—

Further experiments focused on two distinct regions, residues 1690–1721 and 1804–1818, in the A3 domain, responsible for plasmin docking. We have recently demonstrated, in binding-inhibition assays using the plasmin-specific competitor 6-aminohexanoic acid, which directly binds to LBS (21), that the association between plasmin and the factor VIII light chain is mediated by an LBS-dependent mechanism. The known amino acid sequence of the A3 domain indicates that the clustered lysine residues are located in residues 1690–1705 (Lys¹⁶⁹³ and Lys¹⁶⁹⁴) and 1804–1818 (Lys¹⁸⁰⁴, Lys¹⁸⁰⁸, Lys¹⁸¹³, and Lys¹⁸¹⁸), and these two regions are highly conserved in other species (Fig. 6). Therefore, to confirm that these lysine residues confer interactive sites for plasmin, two synthetic peptides derived from sequences 1690–1705 and 1804–1818 were prepared and examined with Ah-plasmin in competitive inhibitory ELISA.

The $^{1649}\text{A3C1C2}$ subunit (120 nM) was incubated with immobilized Ah-plasmin (200 nM) in the presence of increasing concentrations of A3 peptides as described under "Materials and Methods." The results are shown in Fig. 7A. Both the 1690–

Plasmin-interactive Sites in the Factor VIII Light Chain

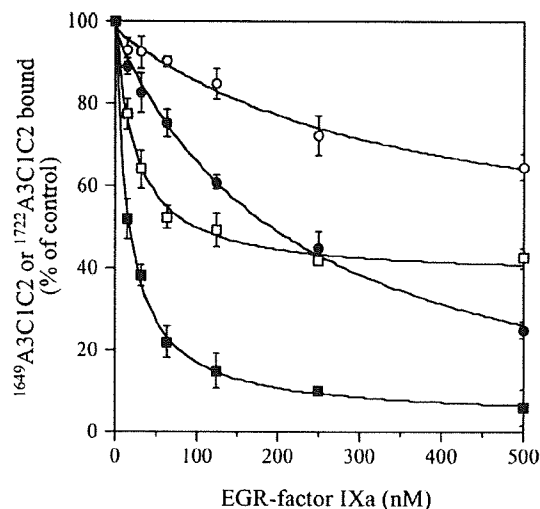


FIGURE 5. Effects of EGR-factor IXa on the binding of the factor VIII light chain to Ah-plasmin in ELISA. $^{1649}\text{A3C1C2}$ (120 nM, open symbols) or $^{1722}\text{A3C1C2}$ (240 nM, closed symbols) was preincubated with varying amounts of EGR-factor IXa for 1 h in the absence (circles symbols) or presence (squares symbols) of phospholipid vesicles (10 μM) prior to reaction with Ah-plasmin (200 nM) immobilized on microtiter wells. Bound A3C1C2 was detected using biotinylated anti-C2 mAb IgG. Absorbance values for A3C1C2 binding to Ah-plasmin in the absence of competitor were considered to represent the 100% level. The percentage of A3C1C2 binding was plotted as a function of EGR-factor IXa concentration, and the plotted data were fitted by nonlinear least squares regression according to Equation 2.

| | 1690 | 1705 | 1804 | 1818 |
|---------|---|-------|--|------|
| human | S F Q K K T R H Y F I A A V E R | ----- | K N F V K P N E T K T Y F W K | |
| porcine | S F Q K R T R H Y F I A A V E Q | ----- | H N F V Q P N E T R T Y F W K | |
| murine | S F Q Q K T R H Y F I A A V E R | ----- | R N F V K P N E T K I Y F W K | |
| canine | S F Q K K T R H Y F I A A V E R | ----- | R K F V N P N E T K I Y F W K | |

FIGURE 6. Sequence alignments of residues 1690–1705 and 1804–1818 for human and other mammalian factor VIII proteins. The sequence shows that the lysine residues (boldface letters) in human are highly conserved across species.

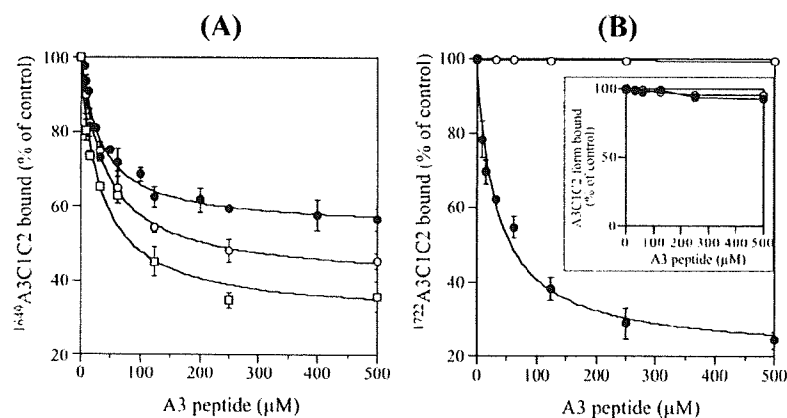


FIGURE 7. Effect of the A3 peptides on the binding of A3C1C2 form to Ah-plasmin in ELISA. $^{1649}\text{A3C1C2}$ (120 nM, A) or $^{1722}\text{A3C1C2}$ (240 nM, B) was mixed with varying concentrations of A3 synthetic peptides and was reacted with Ah-plasmin (200 nM) immobilized on microtiter wells. Bound A3C1C2 was detected using biotinylated anti-C2 mAb IgG. The symbols used are as follows: open circles, 1690–1705 peptide; closed circles, 1804–1818 peptide; open squares, an equimolar mixture of 1690–1705 and 1804–1818 peptides. Inset shows the effect of 1690–1705Ala (open circles) or 1804–1818Ala (closed circles) peptide on $^{1649}\text{A3C1C2}$ or $^{1722}\text{A3C1C2}$ binding to Ah-plasmin, respectively. Absorbance values for A3C1C2 forms binding to Ah-plasmin in the absence of peptide were considered to represent the 100% level. The percentage of A3C1C2 binding was plotted as a function of the A3 peptide concentration, and the plotted data were fitted by nonlinear least squares regression according to Equation 2.

1705 and 1804–1818 peptides blocked the binding of $^{1649}\text{A3C1C2}$ to Ah-plasmin by ~ 55 and $\sim 40\%$, respectively, at the maximum concentration employed (500 μM). The K_i values obtained from curve fitting for the 1690–1705 and 1804–1818 peptides were similar (18.5 ± 3.2 and 20.6 ± 1.5 μM , respectively). Furthermore, an equimolar mixture of both peptides yielded an enhanced inhibitory effect (by $\sim 65\%$) compared with the individual peptides alone, suggesting an additive effect of the two peptides. Similar experiments using the $^{1722}\text{A3C1C2}$ subunit (240 nM) demonstrated that the 1804–1818 peptide blocked the binding of $^{1722}\text{A3C1C2}$ to Ah-plasmin by $\sim 75\%$ with a K_i of 17.3 ± 2.1 μM (Fig. 7B). As expected, the 1690–1705 peptide had little inhibitory effect on this binding.

To further investigate the importance of the lysine residues and/or structural alignments in the two sequences (1690–1705 and 1804–1818), we prepared peptides with scrambled sequences of the same composition and synthesized peptides where the lysine residues were replaced by alanine ($^{1690-1705}\text{Ala}$ and $^{1804-1818}\text{Ala}$, respectively). An equimolar mixture of the scrambled peptide (200 μM) did not inhibit the $^{1649}\text{A3C1C2}$ binding to Ah-plasmin (data not shown). Furthermore, $^{1690-1705}\text{Ala}$ and $^{1804-1818}\text{Ala}$ did not significantly inhibit the binding of $^{1649}\text{A3C1C2}$ or $^{1722}\text{A3C1C2}$ subunits to Ah-plasmin, respectively (Fig. 7B, inset). These results indicated that the lysine residues in the A3 domain, within sequences 1804–1818 and 1690–1705, contribute to the plasmin-interactive sites in the light chain.

Effects of A3 Peptides on Plasmin-catalyzed Cleavage of Lys³⁶ in A1—To further confirm the functional role of residues 1690–1705 and 1804–1818 in plasmin binding, we examined the effects of the A3 peptides on Lys³⁶ cleavage by plasmin. The A1-(1–336)/ $^{1690}\text{A3C1C2}$ dimer (100 nM) was reconstituted with the A2 subunit (300 nM), followed by the addition of plasmin (4 nM) and phospholipid vesicles (10 μM) in the presence of A3 peptides (150 μM). Lys³⁶ cleavage in A1-(1–336), representing the disappearance of A1-(1–336) fragment, was analyzed by Western blotting using an anti-A1 (58.12) IgG in a timed course reaction (Fig. 8A). Change of band density of A1-(1–336) was evaluated by scanning densitometry (Fig. 8B). Compared with the absence of A3 peptide (Fig. 8A, panel a), both individual 1690–1705 and 1804–1818 peptide slightly delayed the disappearance of A1-(1–336) (panels b and c, respectively). Furthermore, in the presence of equimolar amounts of mixture of both peptides, the disappearance of A1-(1–336) was markedly slow, and the band could be observed by $\sim 50\%$ even at 15 min after adding of plasmin, supportive of significant inhibition of plasmin-induced Lys³⁶ cleavage.

Plasmin-interactive Sites in the Factor VIII Light Chain

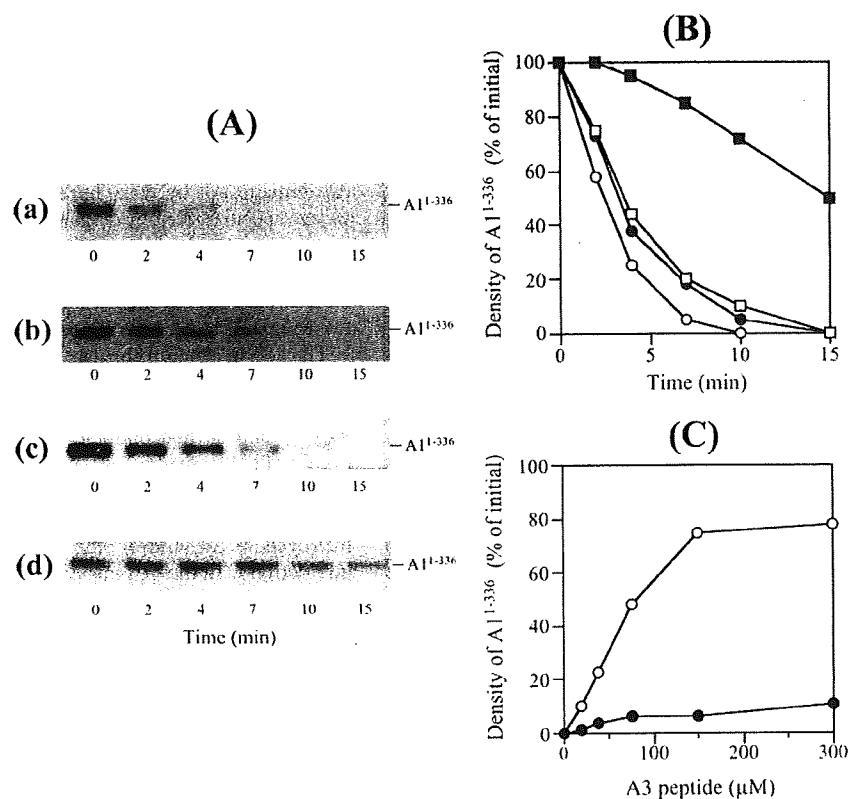


FIGURE 8. Effects of A3 peptides on plasmin-catalyzed cleavage at Lys³⁶ of factor VIIIa with A1¹⁻³³⁶. A, reconstituted A1-(1-336)/¹⁶⁹⁰A3C1C2 dimer (100 nM) reacted with the A2 subunit (300 nM) and phospholipid vesicles (10 μM). Factor VIIIa with A1-(1-336) was incubated with plasmin (4 nM) in the presence of 150 μM A3 peptide (panel a; no peptide, panel b; 1690-1705 peptide, panel c; 1804-1818 peptide, panel d; equimolar mixture of 1690-1705 and 1804-1818 peptides) for the indicated times. Samples were analyzed on 8% gels followed by Western blotting using an anti-A1 (58.12) IgG. B shows quantitative densitometry of A1-(1-336) from blotting data obtained from A. Band density of A1-(1-336) at time 0 was regarded as 100%. The symbols used are as follows: open circles, no peptide; closed circles, 1690-1705 peptide; open squares, 1804-1818 peptide; closed squares, both peptides. C shows the effect of 1690-1705/1804-1818 peptide on plasmin-catalyzed cleavage at Lys³⁶. Various concentrations of 1690-1705/1804-1818 peptide (open circles) or 1690-1705Ala/1804-1818Ala (closed circles) were mixed with factor VIIIa with A1-(1-336), followed by incubation with plasmin (4 nM) for 8 min. Samples were analyzed by Western blotting as above experiments. Density of A1-(1-336) before or after addition of plasmin in the absence of peptide was regarded as 100 or 0%, respectively.

Furthermore, the inhibitory effect of the mixture of 1690-1705 and 1804-1818 peptides showed the dose-dependent manner, and the inhibition effect was ~80% at maximum concentration employed (300 μM) (Fig. 8C). A control experiment using mixture of ¹⁶⁹⁰⁻¹⁷⁰⁵Ala and ¹⁸⁰⁴⁻¹⁸¹⁸Ala peptides showed no significant inhibition (by ~10%). These findings were in keeping with the concept that both the 1690-1705 and 1804-1818 regions in A3 were essential for plasmin docking during factor VIIIa inactivation induced by Lys³⁶ cleavage, although each region interacted separately with the protease.

DISCUSSION

Plasmin inactivates factor VIIIa by proteolysis at specific sites within the heavy and light chains of the activated molecule. We have recently demonstrated that Arg⁴⁸⁴ in the A2 domain of factor VIII significantly contributes to plasmin docking for proteolytic cleavage at Arg³³⁶ in the A1 subunit during enzyme-

catalyzed factor VIIIa inactivation (21). Our present study further revealed that proteolytic cleavage at Lys³⁶ in the A1 domain is supported by plasmin-interactive sites located in the A3 domain of the light chain. This conclusion is based on several novel findings using well established models. (i) The rate for plasmin-catalyzed inactivation of factor VIIIa reconstituted with A1-(1-336) and ¹⁷²¹A3C1C2, reflecting cleavage at Lys³⁶, was reduced by ~55% compared with those with ¹⁶⁴⁹A3C1C2 and ¹⁶⁹⁰A3C1C2. Furthermore, plasmin-catalyzed inactivation of factor VIIIa with A1-(1-336) was significantly inhibited by the addition of exogenous ¹⁶⁹⁰A3C1C2 and rA3, but to a much lesser extent by ¹⁷²¹A3C1C2. (ii) Plasmin cleavage at Lys³⁶ in factor VIIIa with A1/¹⁷²²A3C1C2 dimer was significantly slower than that with A1/¹⁶⁹⁰A3C1C2. (iii) The ¹⁷²²A3C1C2 subunit bound to Ah-plasmin with an ~3-fold weaker affinity than the ¹⁶⁴⁹A3C1C2 or ¹⁶⁹⁰A3C1C2. The rA3 domain bound to Ah-plasmin with similar affinity as ¹⁶⁴⁹A3C1C2, whereas the rC2 domain failed to bind, although a contributory role for the C1 domain in this plasmin binding remains to be completely excluded. (iv) Factor IXa (that binds to the 1804-1818 region) or the A3 peptides (residues 1690-1705 and 1804-1818) competed for light chain binding to Ah-plasmin. (v) The presence of both A3 peptides

inhibited plasmin-catalyzed Lys³⁶ cleavage of factor VIIIa with A1-(1-336) by ~80%. These identified amino acid residues 1690-1705 and 1804-1818 within the A3 domain as essential to plasmin docking for proteolytic cleavage at Lys³⁶.

We observed the partial inactivation of reconstituted factor VIIIa activity with A1-(1-336) or A1-(37-336) by plasmin in this study. Factor Xa generation assay showed that the reconstituted factor VIIIa with truncated A1 forms (A1-(1-336) and A1-(37-336)) retained significant activity, whereas the one-stage clotting assay completely lost these activities (13, 18). This discrepancy can be explained as we described in an earlier report (13). In the factor Xa generation, a K_m value for factor X using factor Xase with native factor VIIIa is ~40 nM, whereas this value is increased 5-fold (K_m ~200 nM) for that with factor VIIIa with A1-(1-336) or A1-(37-336). Because the typical factor Xa generation assay uses concentrations (400 nM) of substrate that yield near V_{max} reaction rates, the rates are inde-

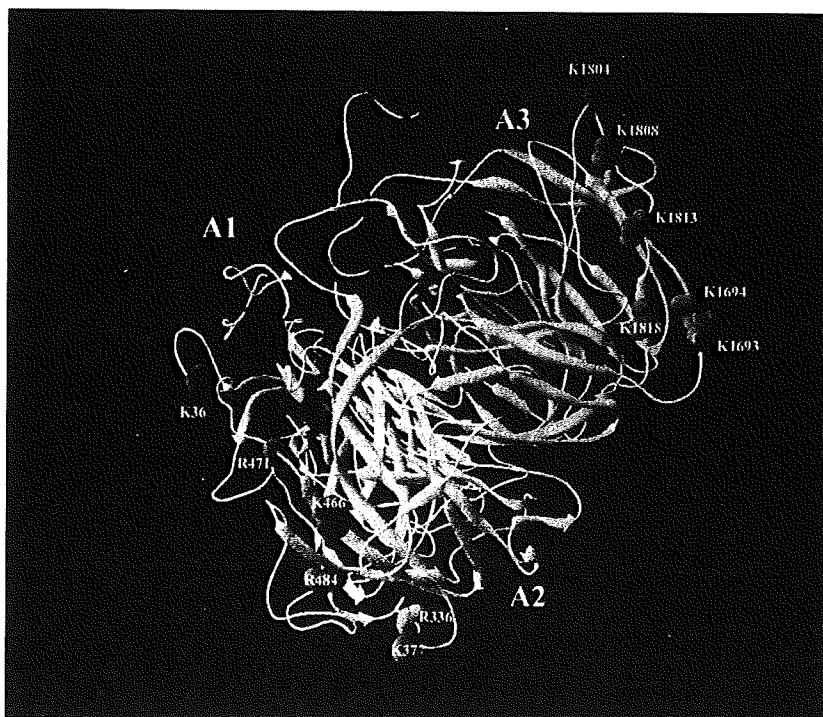


FIGURE 9. Three-dimensional presentation of putative plasmin binding regions in the factor VIII A3 domain based on the ceruloplasmin-based triple A domain model. The A domains (A1–A2–A3 domain) are shown in ribbon format with α -helix in red and β -sheets in yellow. The cleavage sites at Lys³⁶ (magenta) and Arg³³⁶ (gray) are shown in space-filling format. The lysine residues (Lys¹⁶⁹³, Lys¹⁶⁹⁴, Lys¹⁸⁰⁴, Lys¹⁸⁰⁸, Lys¹⁸¹³, and Lys¹⁸¹⁸) within 1690–1705 and 1804–1818 regions that participate in plasmin interaction within the A3 domain are shown in space-filling format (light blue). The A2 residues (Lys³⁷⁷, Lys⁴⁶⁶, Arg⁴⁷¹, and Arg⁴⁸⁴) that contribute to plasmin interaction within the A2 domain (21) are shown in space-filling format (green).

pendent of factor X concentration. However, because the factor X concentration in plasma is ~ 120 nM and this plasma is diluted 4-fold in one-stage clotting assay, the limiting amount of factor X ($\sim 15\%$ of K_m for factor Xase with factor VIIIa with truncated A1 forms) markedly depresses the rate of factor Xase activity, and consequently the A1-(1–336)/A2/A3C1C2 or A1-(37–336)/A2/A3C1C2 loses the factor VIIIa activity in one-stage clotting assay.

Both factor Xa and plasmin inactivate factor VIIIa by cleavage at Arg³³⁶ and Lys³⁶ in the A1 domain (33). An earlier study by Nogami *et al.* (13, 33) revealed that proteolysis by factor Xa at these sites in A1 correlated with inactivation of cofactor function. Close analysis of A1-(1–336) and A1-(37–336) subunits demonstrated inactivation of native factor VIIIa activity by ~ 30 and $\sim 60\%$, respectively, in factor Xa generation assay. Loss of activity resulting from cleavage at Lys³⁶ is associated with an altered molecular conformation that markedly affects the affinity of the A1 subunit for A2 (13). Similarly, factor Xa maximal generation with ¹⁷²¹A3C1C2 subunit in the presence of A1-(37–336) was observed to be $\sim 50\%$ that in the presence of A1-(1–336) (~ 55 and ~ 25 nM/min, respectively), supporting that the N terminus of the A3 domain is unlikely related to associate with the A1 domain. The cleavage rate by factor Xa at Lys³⁶ was > 10 -fold lower than that at Arg³³⁶ (33). Factor Xa-catalyzed cleavage at Lys³⁶, however, is governed by the

A1-(337–372) region, in particular by Asp^{361–363} residues (34), and proteolysis at Arg³³⁶ might interfere with factor Xa docking to the 337–372 region. Cleavage at the identical site by plasmin is regulated by the A3 domain, not by A1. Therefore, we can speculate that Lys³⁶ cleavage by plasmin may be faster than that by factor Xa, although the kinetics on cleavages at both sites by its protease remains to be determined.

The LBS in plasmin consists basically of a cationic center (Lys³⁵ and Arg⁷¹), an anionic center (Asp⁵⁵ and Asp⁵⁷), and a hydrophobic core (Trp⁶², Phe⁶⁴, Trp⁷², and Tyr⁷⁴) (35). The LBS facilitates interaction with substrates and proteins by hydrogen bond and/or ion pair interaction with the cationic or anionic center and van der Waals electronic interaction with the hydrophobic core (36). Recently, we reported that 6-aminohexanoic acid, a specific inhibitor of LBS, blocked interaction between plasmin and the factor VIII light chain by $\sim 90\%$ (21), strongly suggesting that this mechanism is LBS-dependent. Two lysine-rich regions reside in the A3 domain at the N terminus containing Lys¹⁶⁹³ and Lys¹⁶⁹⁴ and in the

mid-section containing Lys¹⁸⁰⁴, Lys¹⁸⁰⁸, Lys¹⁸¹³, and Lys¹⁸¹⁸. We have now identified plasmin-interactive sites in these two regions by competition experiments using synthetic peptides composed of residues 1690–1705 and 1804–1818. Random peptides with scrambled sequences and peptides in which lysine was substituted with alanine failed to compete in the light chain-Ah-plasmin interactions. Our results therefore suggested that lysine residues and structural arrangements within both regions contributed significantly to plasmin docking in the A3 domain.

As noted above, both individual A3 peptides (1690–1705 and 1804–1818) partially inhibited (by $\sim 50\%$) the binding of ¹⁶⁴⁹A3C1C2 to plasmin, and these effects appeared to be additive. In contrast, however, only mixtures of both peptides significantly inhibited plasmin-catalyzed cleavage of functional factor VIIIa at the Lys³⁶ site. These findings were similar to those observed using functional and binding experiments with the ¹⁷²²A3C1C2 subunit. The reasons for the discrepancy between functional and binding assays remain to be fully explored, and studies using modified A3C1C2 in which the 1804–1818 sequence is deleted could be informative. Nevertheless, our data indicate that although each of these regions within the A3 domain interacts separately with plasmin, both are required for plasmin docking and inactivation of procoagulant factor VIIIa mediated by cleavage at Lys³⁶.

Plasmin-interactive Sites in the Factor VIII Light Chain

The factor VIII domain model based on homology with ceruloplasmin (37) describes putative lysine residues, Lys¹⁶⁹³, Lys¹⁶⁹⁴, Lys¹⁸⁰⁴, Lys¹⁸⁰⁸, Lys¹⁸¹³, and Lys¹⁸¹⁸, within residues 1690–1705 and 1804–1818 of the A3 domain, arranged spatially adjacent and exposed on the A3 surface (Fig. 9). This provides an extended surface for plasmin binding, but it is far removed from the cleavage site of Lys³⁶ within the A1 domain. Glu-plasminogen contains five kringle domains and a catalytic domain in a closed form with a radius of gyration of ~40 Å. Conversion to Lys-plasmin by plasminogen activator, however, induces a marked conformational change, termed an open form, with greater flexibility and increased radius of gyration (~60 Å). The dramatic structural alteration enhances high affinity enzyme interactions with protein ligands (38, 39). Molecular mechanisms of this nature could explain the functional relationship between the remote plasmin-interactive sites in A3 and the proteolytic cleavage site at Lys³⁶. In addition, structural modification of the factor VIII light chain bound to plasmin might preferentially support catalysis at Lys³⁶. Interestingly, comparison of amino acid sequences among human, porcine, murine, and canine factor VIII molecules reveals that the two A3 regions are well conserved, supporting the concept that both binding domains are fundamental for protein interactions.

Our study indicated that these functionally essential subunits, involving residues 1690–1705 and 1804–1818 in the A3 domain of factor VIII, constitute a highly basic spacer region exposed on the surface contributing to interaction with plasmin. The 1804–1818 sequence is known to participate in the interaction with at least three proteins, including factor IXa (30), alloantibody inhibitors from multiply transfused hemophilia A patients (40), and low density lipoprotein receptor-related protein that mediates clearance of factor VIII from the circulation (41). Therefore, it is clear that these particular residues play a significant role in the modulation of coagulation reactions by up- and down-regulation of factor VIIIa cofactor function. The 1690–1705 sequence does not seem to have been reported to be involved in other protein interactions.

EGR-factor IXa inhibited factor VIII light chain binding to Ah-plasmin in a solid-phase assay. Furthermore, the presence of phospholipid enhanced the inhibitory effect of EGR-factor IXa and resulted in an ~15-fold decrease of the K_i value for EGR-factor IXa binding. These K_i values were consistent with the K_d values obtained for the light chain-factor IXa interactions observed using a steady-state fluorescein energy transfer fluid assay (25). However, binding stoichiometry for A3C1C2 form and EGR-factor IXa in the presence of phospholipid was unexpectedly different in competition assays. Several possibilities for this reason may be raised. A solid-phase ELISA is a limited assay and is not based on an equilibrium binding. Because the binding affinity for the A3C1C2 of Ah-plasmin is much lower (~15-fold) than that of factor IXa, this difference may affect the competitive inhibition. Furthermore, the A3C1C2 itself bound to factor IXa on the phospholipid membranes may partially affect competitive inhibition, for instance the influence of plasmin binding because of conformational alteration, etc. In addition, the possibility of steric hindrance

because of the EGR molecule of its competitor cannot be excluded. However, the precise reason is unclear at present.

A plasmin-interactive site has been recently identified in the A2 domain within and/or close to a factor IXa-interactive site (21), and in our studies, peptide 1804–1818, representing a factor IXa-interactive site, similarly inhibited the interaction between light chain and Ah-plasmin. Moreover, EGR-factor IXa blocked plasmin-catalyzed inactivation of factor VIIIa in a clotting assay. Therefore, overall the data support that factor IXa, bound to factor VIIIa on the phospholipid surface, might restrict plasmin-induced inactivation of factor VIIIa by occupying the plasmin-interactive sites in the A2 and A3 domains. This mechanism by which factor IXa protects factor VIIIa from plasmin-catalyzed inactivation appears to be similar to that observed with APC-catalyzed inactivation of factor VIIIa (26).

In conclusion, the extended surface of the factor VIII A3 domain, centered on lysine residues in both the 1690–1705 and 1804–1818 regions, contributes to a unique plasmin-interactive site that facilitates plasmin docking during cofactor inactivation by cleavage at Lys³⁶. Our present results further suggest that factor VIII cofactor function is regulated by more complex mechanisms than previously anticipated.

Acknowledgments—We thank Drs. John C. Giddings and Hironao Wakabayashi for helpful suggestions.

REFERENCES

1. Mann, K. G., Nesheim, M. E., Church, W. R., Haley, P., and Krishnaswamy, S. (1990) *Blood* 76, 1–16
2. Wood, W. I., Capon, D. J., Simonsen, C. C., Eaton, D. L., Gitschier, J., Keyt, B., Seeburg, P. H., Smith, D. H., Hollingshead, P., Wion, K. L., Delwart, E., Tuddenham, E. D. G., Vehar, G. A., and Lawn, R. M. (1984) *Nature* 312, 330–337
3. Vehar, G. A., Keyt, B., Eaton, D., Rodriguez, H., O'Brien, D. P., Rotblat, F., Oppermann, H., Keck, R., Wood, W. I., Harkins, R. N., Tuddenham, E. G. D., Lawn, R. M., and Capon, D. J. (1984) *Nature* 312, 337–342
4. Fay, P. J., Anderson, M. T., Chavin, S. L., and Marder, V. J. (1986) *Biochim. Biophys. Acta* 871, 268–278
5. Eaton, D., Rodriguez, H., and Vehar, G. A. (1986) *Biochemistry* 25, 505–512
6. Fay, P. J. (2004) *Blood Rev.* 18, 1–15
7. Fay, P. J., Mastro, M., Koszelak, M. E., and Wakabayashi, H. (2001) *J. Biol. Chem.* 276, 12434–12439
8. Lollar, P., Hill-Eubanks, D. C., and Parker, C. G. (1988) *J. Biol. Chem.* 263, 10451–10455
9. Regan, L. M., and Fay, P. J. (1995) *J. Biol. Chem.* 270, 8546–8552
10. Donath, M. S., Lenting, P. J., van Mourik, J. A., and Mertens, K. (1995) *J. Biol. Chem.* 270, 3648–3655
11. Lamphear, B. J., and Fay, P. J. (1992) *Blood* 80, 3120–3126
12. Koszelak, Rosenblum, M. E., Schmidt, K., Freas, J., Mastro, M., and Fay, P. J. (2002) *J. Biol. Chem.* 277, 11664–11669
13. Nogami, K., Wakabayashi, H., Schmidt, K., and Fay, P. J. (2003) *J. Biol. Chem.* 278, 1634–1641
14. Lapan, K. A., and Fay, P. J. (1997) *J. Biol. Chem.* 272, 2082–2088
15. Bachmann, F. (2000) in *Haemostasis and Thrombosis* (Colman, R. W., ed) 4th Ed., pp. 275–320. Churchill Livingstone, New York
16. Omar, M. N., and Mann, K. G. (1987) *J. Biol. Chem.* 262, 9750–9755
17. Kalafatis, M., and Mann, K. G. (2001) *J. Biol. Chem.* 276, 18614–18623
18. Nogami, K., Shima, M., Matsumoto, T., Nishiya, K., Tanaka, I., and Yoshioka, A. (2007) *J. Biol. Chem.* 282, 5287–5295
19. Samis, J. A., Ramsey, G. D., Walker, J. B., Nesheim, M. E., and Giles, A. R. (2000) *Blood* 95, 943–951

Plasmin-interactive Sites in the Factor VIII Light Chain

20. Pryzdial, E. L., Lavigne, N., Dupuis, N., and Kessler, G. E. (1999) *J. Biol. Chem.* **274**, 8500–8505
21. Nogami, K., Nishiya, K., Saenko, E. L., Takeyama, M., Tanaka, I., Yoshioka, A., and Shima, M. (2008) *Biochim. Biophys. Acta* **1784**, 753–763
22. O'Brien, L. M., Huggins, C. F., and Fay, P. J. (1997) *Blood* **90**, 3943–3950
23. Shima, M., Scandella, D., Yoshioka, A., Nakai, H., Tanaka, I., Kamisue, S., Terada, S., and Fukui, H. (1993) *Thromb. Haemostasis* **69**, 240–246
24. Mimms, L. T., Zampighi, G., Nozaki, Y., Tanford, C., and Reynolds, J. A. (1981) *Biochemistry* **20**, 833–840
25. Jenkins, P. V., Dill, J. L., Zhou, Q., and Fay, P. J. (2004) *Biochemistry* **43**, 5094–5101
26. Regan, L. M., Lamphear, B. J., Huggins, C. F., Walker, F. J., and Fay, P. J. (1994) *J. Biol. Chem.* **269**, 9445–9452
27. O'Brien, L. M., Mastri, M., and Fay, P. J. (2000) *Blood* **95**, 1714–1720
28. Bradford, M. M. (1976) *Anal. Biochem.* **72**, 248–254
29. Pipe, S. W., and Kaufman, R. J. (1997) *Proc. Natl. Acad. Sci. U. S. A.* **94**, 11851–11856
30. Lenting, P. J., van de Loo, J. W., Donath, M. J., van Mourik, J. A., and Mertens, K. (1996) *J. Biol. Chem.* **271**, 1935–1940
31. Takeshima, K., Smith, C., Tait, J., and Fujikawa, K. (2003) *Thromb. Haemostasis* **89**, 788–794
32. Laemmli, U. K. (1970) *Nature* **227**, 680–685
33. Nogami, K., Wakabayashi, H., and Fay, P. J. (2003) *J. Biol. Chem.* **278**, 16502–16509
34. Nogami, K., Lapan, K. A., Zhou, Q., Wakabayashi, H., and Fay, P. J. (2004) *J. Biol. Chem.* **279**, 15763–15771
35. Tulinsky, A., Park, C. H., Mao, B., and Llinas, M. (1988) *Proteins* **3**, 85–96
36. Wu, T. P., Padmanabhan, K., Tulinsky, A., and Mulichak, A. M. (1991) *Biochemistry* **30**, 10589–10594
37. Pemberton, S., Lindley, P., Zaitsev, V., Card, G., Tuddenham, E. G., and Kemball-Cook, G. (1997) *Blood* **89**, 2413–2421
38. Mangel, W. F., Lin, B., and Ramakrishnan, V. (1990) *Science* **248**, 69–73
39. Ramakrishnan, V., Patthy, L., and Mangel, W. F. (1991) *Biochemistry* **30**, 3963–3969
40. Zhong, D., Saenko, E. L., Shima, M., Felch, M., and Scandella, D. (1998) *Blood* **92**, 136–142
41. Bovenschen, N., Boertjes, R. C., van Stempvoort, G., Voorberg, I., Lenting, P. J., Meijer, A. B., and Mertens, K. (2003) *J. Biol. Chem.* **278**, 9370–9377

A modified thrombin generation test for investigating very low levels of factor VIII activity in hemophilia A

Tomoko Matsumoto · Keiji Nogami ·
Kenichi Ogiwara · Midori Shima

Received: 4 September 2009 / Revised: 19 October 2009 / Accepted: 3 November 2009 / Published online: 25 November 2009
© The Japanese Society of Hematology 2009

Abstract Discrepancies between low levels of FVIII:C and clinical symptoms in severe hemophilia A are well-known. We have recently demonstrated that levels of FVIII:C < 0.2 IU/dl were consistent with clinical phenotype by clot waveform analysis, suggesting that precise measurement of very low levels of FVIII:C was clinically important. Thrombin generation tests (TGTs) triggered by tissue factor (TF) have been recently utilized to monitor coagulation function in hemophilia A. We examined whether TGT was useful for evaluating hemophilia A patients with very low levels of FVIII:C. TGTs in 40 hemophilia A plasmas with FVIII:C < 0.2–17 IU/dl (measured by clot waveform analysis using MDA-IITM) were performed using TF and/or ellagic acid (ELG). The lagtime in ELG-TGT at very low levels of FVIII:C was shortened dose-dependently, whilst this parameter in TF-TGT was not significantly affected. Other parameters (endogenous thrombin potential, peak thrombin, time to peak) correlated with FVIII:C levels to some extent in both assays ($r = 0.4$ – 0.7). Using a TF/ELG mixture in TGT, however, the correlation coefficients increased to ~ 0.85 . TGT parameters correlated well with levels of FVIII:C > 0.2 IU/dl, although the lagtime was not especially informative. We conclude that modified TGT, using a TF/ELG mixture as the trigger, is useful for monitoring coagulation function at very low levels of FVIII:C in hemophilia A.

Keywords Hemophilia A · FVIII activity · TGT

1 Introduction

Hemophilia A results from a deficiency or defect in the plasma protein, factor (F)VIII and is the most common of the severe, inherited bleeding disorders. The clinical severity of the disorder generally correlates well with the level of FVIII activity (FVIII:C), and by convention, patients are classified into three clinical categories on the basis of circulating procoagulant activity; severe (FVIII:C < 1.0 IU/dl), moderate (1.0–5.0 IU/dl), and mild (>5.0 IU/dl). The majority of patients in the severe category (undetectable FVIII:C by conventional clotting assays) have frequent spontaneous bleeding episodes unless treated with prophylactic FVIII replacement. Coagulation function in hemophilia A is generally assessed by the measurement of FVIII:C in an activated partial thromboplastin time-assay (aPTT). Some puzzling discrepancies between FVIII:C and bleeding symptoms are well documented, however [1, 2]. In this context, we have previously reported that clot waveform analysis, based on the aPTT, provided additional information on real-time coagulation function in hemophilia A. The temporal parameters in clot waveform analysis, including coagulation velocity and acceleration, appeared to be more relevant to the clinical status than the conventional aPTT alone [3].

More recently, thrombin generation tests (TGT) have been developed to monitor coagulation function in hemophilia A [4, 5]. The TGT provides data on global coagulation by the temporal measurement of thrombin generation, and is generally accepted to be more clinically relevant than specific assays of clotting factors. The concept is based on a cell-based coagulation model [6] in which an enzyme complex of activated FVII (FVIIa) and tissue factor (TF) activates FX (and FIX) and generates of a trace amount of thrombin on cell surfaces at local sites of

T. Matsumoto · K. Nogami (✉) · K. Ogiwara · M. Shima
Department of Pediatrics, Nara Medical University,
840 Shijo-cho, Kashihara Nara 634-8522, Japan
e-mail: roc-noga@naramed-u.ac.jp

endothelial injury (termed the initiation phase). This generated thrombin activates FVIII, FV, and platelets, leading to the formation of tenase and prothrombinase complexes and resulting in a thrombin burst for the conversion of soluble fibrinogen to insoluble fibrin (termed the propagation phase). In hemophilia A, therefore, the reduction in FVIII:C markedly decelerates the thrombin burst during the propagation phase, causing the hemostatic abnormality. In the TGT, the initiation phase is reflected by the lagtime (LT) and the propagation phase is reflected by the parameters peak thrombin (PeakTh), time to peak (ttPeak), and endogenous thrombin potential (ETP) [7, 8]. Thrombin generation in the TGT is usually initiated by the addition of TF/phospholipid (PL) complex. [9].

We have recently reported that although FVIII:C < 1.0 IU/dl is generally used to define severe hemophilia A, precise low levels of FVIII:C (<0.2 IU/dl) were more consistent with this clinical phenotype, suggesting that measurements of very low levels of FVIII:C could be very important to classify clinical status [10]. We anticipated that if the TGT accurately reflects very low levels of FVIII:C, the assay could complement the diagnosis of clinical severity and assist in clinical management. In the present study, therefore, we attempted to optimize the TGT technique for the monitoring of coagulation function in hemophilia A patients with very low levels of FVIII:C.

2 Materials and methods

2.1 Reagents

The reagents, recombinant human TF (rTF; Innovin[®], Dade, Marburg, Germany), and ellagic acid (ELG, Sysmex, Kobe, Japan), a thrombin-specific fluorogenic substrate (Z-Gly-Gly-Arg-AMC, Bachem, Bubendorf, Switzerland) were obtained from the indicated vendors. PL vesicles containing 10% phosphatidylserine, 60% phosphatidylcholine, and 30% phosphatidylethanolamine were prepared as previously described [11]. The thrombin calibrator was obtained from Thrombinoscope (Maastricht, Netherlands). Recombinant FVIII (rFVIII) was a generous gift from Bayer Corp. Japan (Osaka, Japan).

2.2 Plasma samples

Normal pooled plasma was prepared from ten normal healthy individuals. Blood was drawn into evacuated anticoagulant tubes [blood:3.8% (w/v) trisodium citrate, 9:1]. After centrifugation for 15 min at 1,500g, the plasmas were stored at -80°C , and thawed at 37°C immediately prior to the assays. Patients' plasmas were obtained from 40 hemophilia A patients. FVIII:C levels in 12 patients

were <0.2 IU/dl, 6 patients were 0.2–1.0 IU/dl, and 22 patients were 1.0–17.0 IU/dl. FVIII:C levels were measured by clot waveform analysis using MDA-II[™] Hemostasis System. The present studies were performed using blood samples obtained during routine follow-up of patients in the Nara Medical University Hemophilia Program. All samples were obtained with informed consent following local ethical guidelines. Standard samples containing very low levels of FVIII (ranging between 0 and 1.0 IU/dl) were prepared by the addition of known concentrations of rFVIII to congenital FVIII-deficient plasma (George King INC, Overland Park, KS, USA).

2.3 FVIII:C assays

FVIII:C was measured by a one-stage aPTT clotting assay (Thrombocheck APTT-SLA, Sysmex) on the MDA-II[™] Hemostasis System (Trinity Biotech, CW, Ireland) [12]. FVIII-deficient plasma was used as the substrate (Thrombocheck FVIII, Sysmex). A standard curve was prepared using serial dilutions of Coagtrol N plasma (Sysmex) (1:10–1:5, 120) in 50 mM imidazole saline buffer (pH 7.3). Each test sample was diluted 1:10 and 1:20 in imidazole saline buffer.

2.4 Thrombin generation assay

The TGT was measured using a modification of the method reported by Hemker et al. [9]. Briefly, 20 μl trigger reagent (TF/PL or ELG) and 80 μl test plasma were mixed in 96-well round-bottom microtiter plates (Immulon2HB U bottom plate; ThermoLab System, Helsinki, Finland). The plate was placed in the fluorometer and allowed to warm to 37°C for 10 min. The dispenser of the fluorometer was flushed with 20 μl warmed 100 mM CaCl_2 and 5 mM fluorogenic substrate Z-Gly-Gly-Arg-AMC. At the start of the assay, 20 μl of CaCl_2 and fluorogenic substrate was dispensed to all wells to be measured. The development of a fluorescent signal was monitored at 8-s intervals using a Fluoroskan Ascent microplate reader (Thermo Electron Co., Waltham, MA, USA) with a 390-nm (excitation) and 460-nm (emission) filter set. Thrombin generation (in nM) was calculated from Fluorescent signals corrected by reference to the thrombin calibrator samples. Data analyses were performed using Thrombinoscope software. The parameters, LT, ETP, PeakTh, and ttPeak, were recorded.

2.5 Data analyses

Measurements were obtained in several separate assays as indicated, and the mean and standard deviation are shown. Correlations between the four parameters in the TGT and

FVIII:C were determined using Spearman's correlation test.

3 Results

3.1 TF-trigger TGT (TF-TGT) in hemophilia A plasmas

For assessing coagulation function in hemophilia A, the TGT has been generally performed using a mixture of TF/PL complex as the initiation trigger [9]. In the present study we utilized a mixture of TF/PL at concentrations of 0.5 μM and 4 μM , respectively. Figure 1a illustrates a representative thrombogram observed in normal plasma and hemophilia A plasma (FVIII:C < 0.2 IU/dl). The TGT parameters obtained from normal plasma were LT, 6.3 ± 1.1 min; ETP, $2,771 \pm 1,124$ nM min; PeakTh, 203 ± 53 nM; and ttPeak, 15.2 ± 2.9 min. In hemophilia A, these parameters were 6.2 ± 1.5 min, 677 ± 403 nM min, 62.0 ± 16.7 nM, and 26.8 ± 4.4 min, respectively, showing significant differences in thrombin generation but no difference in LT. We further examined the relationship between FVIII:C levels (by one-stage clotting assay) and TF-TGT in hemophilia A. FVIII:C levels in the 40 hemophilia A plasmas ranged from <0.2 to 17.0 IU/dl. The ETP (Fig. 1, panel C) and PeakTh (panel D) correlated with FVIII:C levels to some extent ($r = 0.689$ and 0.628 , respectively). The LT (panel B) and ttPeak (panel E) correlated less well with FVIII:C ($r = 0.220$ and 0.417 , respectively).

In order to evaluate the relationship between very low levels of FVIII:C and the TF-TGT, serial dilutions of rFVIII were added to commercial FVIII-deficient plasma.

Significant differences between ascending concentration pairs were determined by analysis described in Sect. 2. There were no significant differences in adjoining values at any concentrations <1.6 IU/dl (Table 1A). The lowest limit of FVIII:C detected by this method was 3.2 IU/dl, confirming the relative insensitivity of the method to reflect low levels of FVIII:C.

3.2 ELG-trigger TGT (ELG-TGT) in hemophilia A plasmas

The contact activation factor, ELG, was used as an alternative initiation trigger in TGT. ELG is known to replicate glass activation of FIXa in the intrinsic coagulation system [13]. In control experiments, thrombin generation obtained in the presence of ELG was dose-dependent, and the reaction was shown to be saturated and optimal at a concentration of 0.3 μM (data not shown). ELG was used in the present study, therefore, at a concentration of 0.3 μM . Figure 2a illustrates a representative thrombogram observed in normal plasma and hemophilia A plasma (FVIII:C < 0.2 IU/dl). TGT parameters using normal plasma were LT, 9.9 ± 1.6 min; ETP, $3,197 \pm 545$ nM min; PeakTh, 425 ± 48 nM; and ttPeak, 13.0 ± 2.4 min, indicating that thrombin generation in the ELG-TGT was greater than that in the TF-TGT. In contrast, the ELG-TGT failed to respond to this low level of FVIII:C.

Analyses of ELG-TGT and FVIII:C in hemophilia A demonstrated that ETP (Fig. 2, 0 C), PeakTh (panel D), and ttPeak (panel E) correlated with FVIII:C to similar or greater degree ($r = 0.645$, 0.690 , and 0.669 , respectively) compared to the data obtained in the TF-TGT. The LT (panel B) also correlated reasonably well with FVIII:C

Fig. 1 TF-TGT in hemophilia A. **a** Mixtures of TF and PL (f.c. 0.5 μM and 4 μM) were added to normal plasma (line 1) or hemophilia A plasma (FVIII:C < 0.2 IU/dl, line 2) prior to evaluating thrombin generation. Representative thrombograms are illustrated in **a**. **b–e** Correlations between various FVIII:C levels and TGT parameters (LT, ETP, PeakTh, and ttPeak, respectively) obtained in 40 hemophilia A patients. The coefficient variation (CV) of all parameters obtained by this assay showed <10%

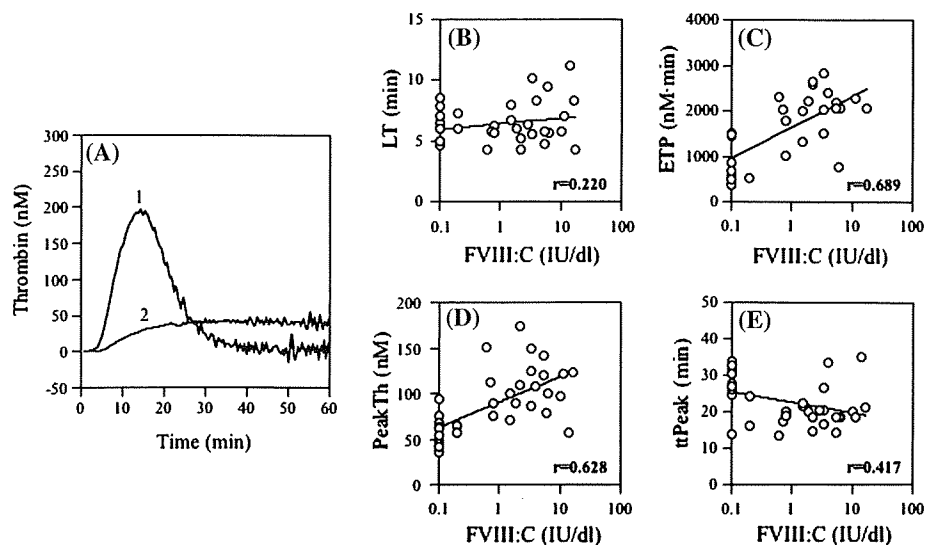


Table 1 Parameters of TF-TGT or ELG-TGT at various concentrations of rFVIII**(A) TF-TGT**

| TGT parameters | FVIII:C (IU/dl) | | | | | | |
|----------------|-----------------|------------|------------|------------|------------|------------|------------|
| | 0 | 0.1 | 0.2 | 0.4 | 0.8 | 1.6 | 3.2 |
| LT (min) | 5.8 ± 1.0 | 5.9 ± 1.1 | 5.9 ± 1.1 | 5.9 ± 1.1 | 5.9 ± 1.1 | 5.7 ± 0.6 | 5.8 ± 0.6 |
| P value | ← n.d. → | ← n.d. → | ← n.d. → | ← n.d. → | ← n.d. → | ← n.d. → | ← n.d. → |
| ETP (nM·min) | 1768 ± 92 | 1790 ± 165 | 1822 ± 115 | 1834 ± 101 | 1903 ± 108 | 2016 ± 86 | 2222 ± 159 |
| P value | ← n.d. → | ← n.d. → | ← n.d. → | ← n.d. → | ← n.d. → | ← n.d. → | ← n.d. → |
| PeakTh (nM) | 81.5 ± 6.7 | 76.8 ± 5.2 | 79.6 ± 4.4 | 81.8 ± 6.1 | 85.5 ± 6.0 | 89.1 ± 2.8 | 95.8 ± 7.2 |
| P value | ← n.d. → | ← n.d. → | ← n.d. → | ← n.d. → | ← n.d. → | ← n.d. → | ← p<0.05 → |
| ttPeak (min) | 27.0 ± 2.5 | 27.0 ± 2.3 | 26.0 ± 1.7 | 25.6 ± 1.7 | 24.4 ± 1.5 | 23.4 ± 1.6 | 20.2 ± 1.8 |
| P value | ← n.d. → | ← n.d. → | ← n.d. → | ← n.d. → | ← n.d. → | ← n.d. → | ← p<0.05 → |

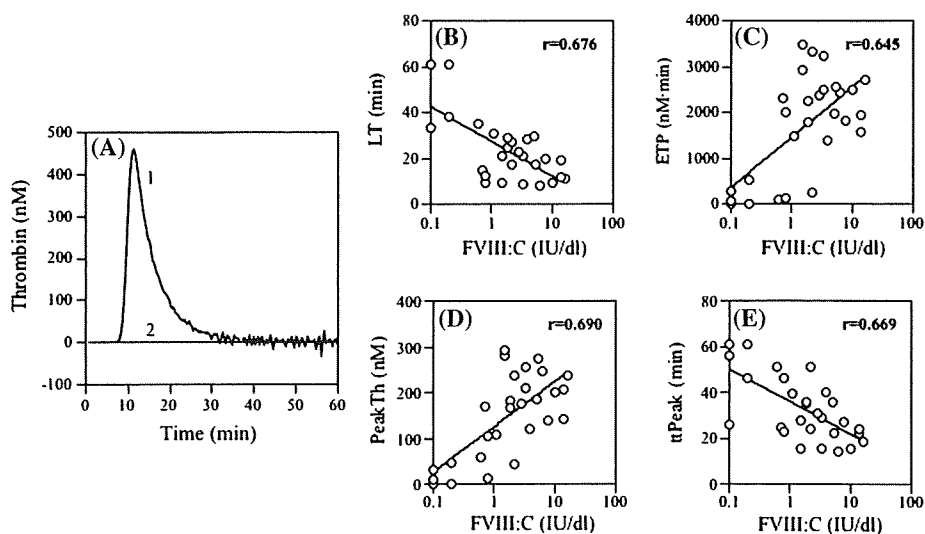
(B) ELG-TGT

| TGT parameters | FVIII:C (IU/dl) | | | | |
|----------------|-----------------|------------|------------|-------------|------------|
| | 0 | 0.1 | 0.2 | 0.4 | 0.8 |
| LT (min) | >60 | 24.5 ± 3.5 | 19.3 ± 1.6 | 16.1 ± 1.0 | 14.2 ± 1.0 |
| P value | ← p<0.01 → | ← p<0.05 → | ← p<0.05 → | ← p<0.05 → | ← p<0.05 → |
| ETP (nM·min) | 0 | 180 ± 28 | 540 ± 98 | 1626 ± 191 | 2302 ± 162 |
| P value | ← p<0.01 → | ← p<0.01 → | ← p<0.01 → | ← p<0.01 → | ← p<0.01 → |
| PeakTh (nM) | 0 | 22.5 ± 5.3 | 47.5 ± 9.3 | 82.2 ± 12.7 | 127 ± 14 |
| P value | ← p<0.01 → | ← p<0.01 → | ← p<0.01 → | ← p<0.01 → | ← p<0.01 → |
| ttPeak (min) | >60 | 47.4 ± 4.8 | 37.9 ± 2.9 | 29.9 ± 2.1 | 25.2 ± 1.4 |
| P value | ← p<0.01 → | ← p<0.01 → | ← p<0.01 → | ← p<0.01 → | ← p<0.01 → |

Various concentrations of rFVIII were added to FVIII-deficient plasmas, and TGT of samples were performed as described in Sect. 2. The measurements were performed at ten separate times, and the average and standard deviation values were shown

n.d. No difference

Fig. 2 ELG-TGT in hemophilia A. **a** ELG (f.c. 0.3 μM) was added to normal plasma (line 1) or hemophilia A plasma (FVIII:C < 0.2 IU/dl, line 2) prior to evaluating thrombin generation. Representative thrombograms are illustrated in **a**. **b–e** Correlations between FVIII:C levels and TGT parameters (LT, ETP, PeakTh, and ttPeak, respectively) obtained in 40 hemophilia A patients. The CV of all parameters obtained by this assay showed <10%



level ($r = 0.676$). Significant differences of adjoining values were demonstrated in all ELG-TGT parameters at low levels of FVIII:C even at concentrations <0.1 IU/dl

(Table 1B). The lowest limit of sensitivity of FVIII:C by this method was <0.1 IU/dl. In addition, the LT strongly depended on FVIII:C levels indicating that this method

poorly reflected the initiation phase on the coagulation process in the cell-based model.

3.3 TF/ELG-trigger TGT (TF/ELG-TGT) in hemophilia A

The above results suggested that neither the TF-TGT nor the ELG-TGT was likely to be informative in the clinical management patients with very low levels of FVIII:C. We assessed, therefore, the TGT using a mixture of TF/PL (0.5 pM/4 μ M) and ELG (0.3 μ M) in order to compensate for the apparent disadvantages of the separate assays. Figure 3a illustrates a representative thrombogram observed in normal plasma and severe hemophilia A. The TGT parameters obtained in normal plasma were 4.5 ± 0.3 min (LT), $3,140 \pm 480$ nM min (ETP), 370 ± 33 nM (PeakTh), and 8.2 ± 0.9 min (ttPeak). In hemophilia A, the parameters were 4.6 ± 0.8 min, $1,095 \pm 464$ nM min, 64.0 ± 14.1 nM, and 27.3 ± 9.8 min, respectively. The results indicated that the range of generated thrombin was greater than that in TF-TGT and that the LT was unchanged and PeakTh was moderated in severe hemophilia A patient.

Analyses of the TGT parameters and FVIII:C levels in hemophilia A demonstrated that ETP (Fig. 3, panel C), PeakTh (panel D), and ttPeak (panel E) correlated with FVIII:C levels to a much greater extent ($r = 0.858, 0.857,$ and 0.849 , respectively) than that obtained in the separate assays. Of particular note, the LT (panel B) was poorly related to FVIII:C. On the limit for low level of FVIII:C, evaluated by TF/ELG-TGT, significant differences of the adjoining values were not observed at LT and ETP at concentration of <0.8 IU/dl (Table 2), while they were observed at PeakTh ($P < 0.01$) and ttPeak ($P < 0.05$) at >0.2 IU/dl. The lowest limit of sensitivity for FVIII:C in

this assay was 0.2 IU/dl and was similar to that for clot waveform analysis reported by Matsumoto et al. [14]. Furthermore, the presence of corn trypsin inhibitor (CTI) in this assay did not show significant differences ($P > 0.05$) for all parameters, compared to its absence (data not shown).

We previously demonstrated that very low levels of FVIII:C (lowest limit 0.2 IU/dl) could be evaluated by clot waveform analysis and FVIII:C < 0.2 IU/dl was significantly consistent with clinical severe phenotype of hemophilia A [14]. Therefore, we compared with the parameters of TF/ELG-TGT and clot waveform analysis in hemophilia A patients with FVIII:C < 1.0 IU/dl. Both parameters of PeakTh and ttPeak in TGT highly ($r = 0.73$ – 0.83) correlated with both parameters of clot time and lmin 2l in clot waveform analysis (Table 3), supporting that even TF/ELG-TGT could fully evaluate very low levels of FVIII:C and clinical severity in hemophilia A patients.

Taken together, these findings demonstrated that the TF/ELG-TGT could provide valuable information for monitoring the coagulation mechanism based on cell-based reactions in patients with very low levels of FVIII:C (>0.2 IU/dl).

4 Discussion

We have demonstrated that a modification of the TGT assay to include TF/ELG to initiate thrombin generation accurately reflects coagulation function in hemophilia A patients with very low levels of FVIII:C. Several groups [5, 15, 16] have previously reported that TGT assays using low concentrations of TF (0.5–1.0 pM) and PL (4 μ M) generally correlate with FVIII:C, although the effectiveness of

Fig. 3 TF/ELG-TGT in hemophilia A. **a** Mixtures of TF/PL and ELG (f.c. 0.5 pM/4 and 0.3 μ M) were added to normal plasma (line 1) or hemophilia A plasma (FVIII:C < 0.2 IU/dl, line 2) prior to evaluating thrombin generation. Representative thrombograms are illustrated in **a**. **b–e** Correlations between FVIII:C levels in and TGT parameters (LT, ETP, PeakTh, and ttPeak, respectively) obtained in hemophilia A patients. The CV of all parameters obtained by this assay showed $<10\%$

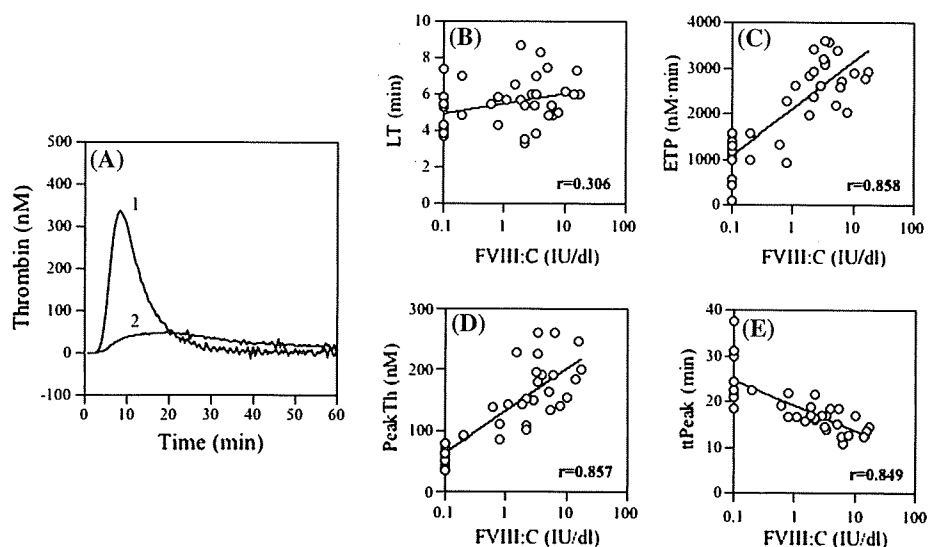


Table 2 Parameters of TF/ELG-TGT at various concentrations of rFVIII

| TGT parameters | FVIII:C (IU/dl) | | | | |
|----------------|---|------------|------------|------------|------------|
| | 0 | 0.1 | 0.2 | 0.4 | 0.8 |
| LT (min) | 4.5 ± 0.1 | 4.6 ± 0.2 | 4.7 ± 0.2 | 4.8 ± 0.3 | 4.9 ± 0.3 |
| <i>P</i> value | ← n.d. → | | | | |
| ETP (nM·min) | 2571 ± 109 | 2572 ± 74 | 2572 ± 63 | 2581 ± 49 | 2606 ± 24 |
| <i>P</i> value | ← n.d. → | | | | |
| PeakTh (nM) | 139 ± 8 | 140 ± 8 | 142 ± 9 | 157 ± 7 | 176 ± 2 |
| <i>P</i> value | ← n.d. → ← n.d. → ← <i>p</i> <0.01 → ← <i>p</i> <0.01 → | | | | |
| ttPeak (min) | 15.2 ± 0.5 | 15.8 ± 0.8 | 15.7 ± 0.9 | 14.6 ± 0.6 | 13.8 ± 0.4 |
| <i>P</i> value | ← n.d. → ← n.d. → ← <i>p</i> <0.05 → ← <i>p</i> <0.05 → | | | | |

Various concentrations of rFVIII were added to FVIII-deficiency plasmas, and TGT of samples were performed as described in Sect. 2. The measurements were performed at ten separate times, and the average and standard deviation values were shown

n.d. No difference

Table 3 Correlation between the parameters of TF/ELG-TGT and clot waveform analysis in hemophilia A patients with FVIII:C < 1.0 IU/dl

| TF/ELG-TGT | Clot waveform analysis Clot time (sec) | <i>r</i> min 2l |
|--------------|---|-----------------|
| LT (min) | 0.050 | 0.053 |
| ETP (nM·min) | -0.532 | 0.598 |
| PeakTh (nM) | -0.768 | 0.734 |
| ttPeak (min) | 0.829 | -0.798 |

Values show the correlation coefficient between each parameter obtained in both assays

the method in the presence of very low levels of FVIII:C remains to be established. In the present study, low concentrations of TF mediated modest thrombin generation in normal plasma, and differences in PeakTh and ETP (reflecting the propagation phase) between normal and hemophilia A plasma were not markedly significant. It is generally accepted that the spontaneous hemorrhagic symptoms in severe hemophilia A are caused by relatively minor amounts of TF in joints and muscles [17] resulting in defective activation of the initiation phase by FVIIa/TF complex. In the present investigation, however, the LT, reflecting the initiation phase, was not especially sensitive to very low levels of FVIII:C (<1.0 IU/dl) and this parameter was not useful for assessing precise coagulation function in these circumstances.

Several studies have utilized the TF-TGT to evaluate replacement therapy in hemophilia A. Variable TGT parameters have been described in patients with similar levels of FVIII:C, and different ranges of ETP values have been demonstrated even in control individuals with normal levels of FVIII:C [4, 18]. Furthermore, Beltran-Miranda et al. [5] reported that although there was a reasonably

good correlation between clinical severity and PeakTh in hemophilia A, overall, the TF-TGT did not offer any advantages for the evaluation of clinical severity compared to the measurement of FVIII:C by one-stage clotting assay. In addition, as discussed earlier, little information is available on the use of the TGT for assessing very low levels of FVIII:C.

McIntosh et al. [13] reported that the TGT triggered by FIXa reflected coagulation function at low levels of FVIII:C. In aPTT-based assays, soluble ELG is widely used as an activator of intrinsic coagulation. In the present study we also used ELG for the following reasons: (1) thrombin generation using ELG gave similar results to those using FIXa (data not shown), (2) other coagulation disorders as well as hemophilia A can be evaluated, and (3) it is cost-effective. We demonstrated that the ELG-TGT provided a sensitive index of coagulation function even at very low levels of FVIII:C. This assay showed the difference of lowest limit of FVIII:C (0.2 and <0.1 IU/dl, respectively) in plasmas of hemophilia A patients and samples prepared by the addition of rFVIII to FVIII-deficient plasma. This discrepancy may be explained by the difference of amounts of other blood coagulation factors except for FVIII containing in plasmas of hemophilia A patients. However, in ELG-TGT, the LT was again dependent on the presence of FVIII:C, and this parameter failed to quantify coagulation function in the cell-based coagulation model.

The aforementioned findings prompted us, therefore, to design a method based on a mixture of TF/PL and ELG. Under these conditions, the LT was little affected independently of FVIII:C, and differences in thrombin generation between normal individuals and hemophilia A was strikingly more evident than that in TF-TGT. Significantly higher correlations (*r* > 0.85) between FVIII:C and TGT parameters were observed in hemophilia A patients and the

findings indicated that the TF/ELG-TGT could be a useful technique to examine both the initiation phase and the propagation phase of cell-based coagulation function. Moreover, the sensitivity of the method to very low levels of FVIII:C was approximately 0.2 IU/dl, similar to that observed using clot waveform analysis [14]. The TGT parameters were more variable than those seen in the aPTT-based assay, however, and may have depended on the concentration of coagulation factors other than FVIII:C in the plasma samples. Nevertheless, the TF/ELG-TGT provided good data for the classification of clinical severity in patients with very low levels of FVIII:C.

The CTI is often used in TF-TGT to block the activation of contact pathway and to have little influence of parameter LT, reflecting the initiation phase [19]. Although, in particular, the addition of CTI appears to be preferred in TF-TGT using a low concentration (1 pM) of TF [20], the effects of CTI by TF-TGT at very low levels of FVIII:C have remained to be investigated. The presence of CTI in TF/ELG-TGT, however, did not significantly affect all parameters, compared to its absence (data not shown), supporting that CTI would not be required for evaluation of coagulation function on very low levels of FVIII:C in this assay, although this reason is unclear at this present. Therefore, we conclude that in TF/ELG-TGT, the initiation trigger is due to TF/FVIIa, based on little change of LT, and the presence of ELG causes more enhancing activation of intrinsic coagulation; consequently, this assay can possess the higher sensitivity for coagulation function of hemophilia A with very low levels of FVIII:C.

Acknowledgment This work was partly supported by grants for MEXT KAKENHI 21591370 and The Mother and Child Health Foundation. We thank Dr. John. C. Giddings for helpful suggestions.

References

- van den Berg HM, De Groot PH, Fischer K. Phenotypic heterogeneity in severe hemophilia. *J Thromb Haemost.* 2007;5:151–6.
- Trossaert M, Regnault V, Sigaud M, Boisseau P, Fressinaud E, Lecompte T. Mild hemophilia with factor VIII assay discrepancy: using thrombin generation assay to assess the bleeding phenotype. *J Thromb Haemost.* 2008;6:486–93.
- Shima M, Matsumoto T, Fukuda K, Kubota Y, Tanaka I, Nishiyama K, et al. The utility of activated partial thromboplastin time (aPTT) clot waveform analysis in the investigation of hemophilia A patients with very low levels of factor VIII activity (FVIII:C). *Thromb Haemost.* 2002;87:436–41.
- Siegemund T, Petros S, Siegemund A, Scholz U, Engelmann G. Thrombin generation in severe hemophilia A and B: the endogenous thrombin potential in platelet-rich plasma. *Thromb Haemost.* 2003;90:781–7.
- Beltrán-Miranda CP, Khan A, Jaloma-Cruz AR, Laffan MA. Thrombin generation and phenotypic correlation in haemophilia A. *Haemophilia.* 2005;11:326–34.
- Hoffman M. A cell-based model of coagulation and the role of factor VIIa. *Blood Rev.* 2003;17:1–5.
- Hemker HC, Giesen P, Al Dieri R, Regnault V, de Smed E, Wagenvoort R, et al. The calibrated automated thrombogram (CAT): a universal routine test for hyper- and hypocoagulability. *Pathophysiol Haemost Thromb.* 2002;32:249–53.
- Barrowcliffe TW, Cattaneo M, Podda GM, Bucciarelli P, Lussana F, Lecchi A, et al. New approaches for measuring coagulation. *Haemophilia.* 2006;12:76–81.
- Hemker HC, Giesen P, Al Dieri R, Regnault V, de Smed E, Wagenvoort R, et al. Calibrated automated thrombin generation measurement in clotting plasma. *Pathophysiol Haemost Thromb.* 2003;33:4–15.
- Shima M, Matsumoto T, Ogiwara K. New assays for monitoring haemophilia treatment. *Haemophilia.* 2008;14:83–92.
- Okuda M, Yamamoto Y. Usefulness of synthetic phospholipids in measurement of activated partial thromboplastin time: a new preparation procedure to reduce batch difference. *Clin Lab Haematol.* 2004;26:215–23.
- Braun PJ, Given TB, Stead AG, Beck LR, Gooch SA, Swan RJ, et al. Properties of optical data from activated partial thromboplastin time and prothrombin time assay. *Thromb Haemost.* 1997;78:1079–87.
- McIntosh JH, Owens D, Lee CA, Raunt S, Barrowcliffe TW. A modified thrombin generation test for the measurement of factor VIII concentrates. *J Thromb Haemost.* 2003;1:1005–11.
- Matsumoto T, Shima M, Takeyama M, Yoshida K, Tanaka I, Sakurai Y, et al. The measurement of low levels of factor VIII or factor IX in hemophilia A and hemophilia B plasma by clot waveform analysis and thrombin generation assay. *J Thromb Haemost.* 2006;4:377–84.
- Dargaud Y, Béguin S, Lienhart A, Dieri RA, Trzeciak C, Bordet JC, et al. Evaluation of thrombin generating capacity in plasma from patients with haemophilia A and B. *J Thromb Haemost.* 2005;93:475–80.
- Lewis SJ, Stephens E, Florou G, Macartney NJ, Hathaway LS, Knipping J, et al. Measurement of global haemostasis in severe haemophilia A following factor VIII infusion. *Br J Haematol.* 2007;138:775–82.
- Pawlinski R, Fernandes A, Kehrlé B, Pedersen B, Parry G, Erlich J, et al. Tissue factor deficiency causes cardiac fibrosis and left ventricular dysfunction. *Proc Natl Acad Sci USA.* 2002;99:15333–8.
- van Veen JJ, Gatt A, Makris M. Thrombin generation testing in routine clinical practice. *Br J Haematol.* 2008;142:889–903.
- Dargaud Y, Bordet JC, Francillon S, Négrier C. Haemophilia patients exhibit prolonged coagulation time but normal lag time of thrombin generation test. *Thromb Haemost.* 2007;97:675–6.
- van Veen JJ, Gatt A, Cooper PC, Kitchen S, Bowyer AE, Makris M. Corn trypsin inhibitor in fluorogenic thrombin-generation measurements is only necessary at low tissue factor concentrations and influences the relationship between factor VIII coagulant activity and thrombogram parameters. *Blood Coagul Fibrin.* 2008;19:183–9.